OPEN ACCESS

KING'S College LONDON

King's Research Portal

Document Version
Peer reviewed version

Link to publication record in King's Research Portal

Citation for published version (APA):
So, C. W. E., Zeisig, B., Fung, T. K., Zarowiecki, M., Stanojevic, B., Lynn, C., & Mufti, G. (in press). Functional reconstruction of human AML reveals stem cell origin and vulnerability of treatment resistant MLL-rearranged leukemia. *Science Translational Medicine*.

Citing this paper
Please note that where the full-text provided on King's Research Portal is the Author Accepted Manuscript or Post-Print version this may differ from the final Published version. If citing, it is advised that you check and use the publisher's definitive version for pagination, volume/issue, and date of publication details. And where the final published version is provided on the Research Portal, if citing you are again advised to check the publisher's website for any subsequent corrections.

General rights
Copyright and moral rights for the publications made accessible in the Research Portal are retained by the authors and/or other copyright owners and it is a condition of accessing publications that users recognize and abide by the legal requirements associated with these rights.

•Users may download and print one copy of any publication from the Research Portal for the purpose of private study or research.
•You may not further distribute the material or use it for any profit-making activity or commercial gain
•You may freely distribute the URL identifying the publication in the Research Portal

Take down policy
If you believe that this document breaches copyright please contact librarypure@kcl.ac.uk providing details, and we will remove access to the work immediately and investigate your claim.

Download date: 13. May. 2025

Functional reconstruction of human AML reveals stem cell origin and vulnerability of treatment-resistant MLL-rearranged leukemia

Bernd B Zeisig[1,2]*, Tsz Kan Fung[1,2]*, Magdalena Zarowiecki[1]ϕ, Chiou Tsun Tsai[1], Huacheng Luo[3], Boban Stanojevic[1,4], Claire Lynn[1]Ψ, Anskar YH Leung[5], Jan Zuna[6], Marketa Zaliova[6], Martin Bornhauser[7], Malte von Bonin[7], Boris Lenhard[8], Suming Huang[3]§, Ghulam J Mufti[1,2], Chi Wai Eric So[1,2,9]§

1. Leukaemia and Stem Cell Biology Group, School of Cancer and Pharmaceutical Sciences, King's College London, SE5 9NU
2. Department of Haematological Medicine, King's College Hospital, SE5 9RS
3. Division of Pediatric Hematology/Oncology, Department of Pediatrics, Penn State Cancer Institute, Pennsylvania State University College of Medicine, Hershey, PA 17033
4. Laboratory for Radiobiology and Molecular Genetics, Vinca Institute of Nuclear Science, University of Belgrade, 11000 Belgrade, Serbia
5. Department of Medicine, The University of Hong Kong, Pokfulam Road, HKSAR, China
6. CLIP, Department of Paediatric Haematology and Oncology, 2nd Faculty of Medicine, Charles University and University Hospital Motol, 150 06 Prague 5, Czech Republic
7. Department of Medicine, University Hospital, 01307 Dresden, Germany
8. Institute of Clinical Sciences, Faculty of Medicine, Imperial College London, London W12 0NN, UK; Computational Regulatory Genomics, MRC London Institute of Medical Sciences, London W12 0NN, UK; Sars International Centre for Marine Molecular Biology, University of Bergen, N-5008 Bergen, Norway.

ϕcurrent address: Genomics England, Queen Mary University of London, EC1M 6BQ

Ψcurrent address: Evolutionary Genomics and Modelling, Department of Molecular Pathology, Institute of Cancer Research, SW7 3RP

*equal contribution

§corresponding author

[9]Lead contact:

Chi Wai Eric So, Leukaemia and Stem Cell Biology Group, School of Cancer and Pharmaceutical Sciences, King's College London, SE5 9NU

Email: eric.so@kcl.ac.uk

One Sentence Summary:

Chemoresistant human $CD34^{-/lo}/CD38^{+}$ MLL leukemic stem cells originate from HSCs and can be re-sensitized by targeting ABCC3 with fidaxomicin.

Abstract

Chemoresistance remains the major challenge for successful treatment of acute myeloid leukemia (AML). Although recent mouse studies suggest that treatment response of genetically and immunophenotypically indistinguishable AML can be influenced by their different cells of origin, corresponding evidence in human disease is still largely lacking. By combining prospective disease modeling using highly purified human hematopoietic stem or progenitor cells with retrospective deconvolution study of leukemia stem cells (LSCs) from primary patient samples, we identified human hematopoietic stem cells (HSCs) and common myeloid progenitors (CMPs) as two distinctive origins for human AML driven by *Mixed Lineage Leukemia* (*MLL*) gene fusions (MLL-AML). Despite LSCs from either MLL-rearranged HSCs or MLL-rearranged CMPs having a mature $CD34^{-/lo}/CD38^{+}$ immunophenotype in both the humanized model and primary patient samples, the resulting AML cells exhibited contrasting responses to chemotherapy. HSC-derived MLL-AML was highly resistant to chemotherapy and expressed elevated amounts of the multispecific anion transporter ABCC3. Inhibition of ABCC3 by shRNA-mediated knockdown or with a small molecule inhibitor, fidaxomicin currently used for diarrhea associated with *Clostridium difficile* infection, effectively re-sensitized HSC-derived MLL-AML towards standard chemotherapeutic drugs. This study not only functionally established two distinctive origins of human LSCs for MLL-AML and their role in mediating chemoresistance, but also identified a potential therapeutic avenue for stem cell-associated treatment resistance by repurposing a well-tolerated anti-diarrhea drug already used in the clinic.

Introduction

Chemoresistance is a major clinical challenge for acute myeloid leukemia (AML) treatment and is often mediated by leukemia stem cells (LSCs) (*1*). Although specific genetic mutations have been instrumental in guiding treatment regimens, heterogeneous responses are still observed even within genetically homogeneous subgroups, including those driven by gene fusions involving *mixed lineage leukemia* (*MLL)* (collectively referred to as MLL-AML), suggesting that non-genetic drivers cause the observed functional heterogeneity (*2, 3*). AML can arise from different progenitor populations, which could contribute to the heterogenous responses of the cells. Therefore, identification of the origins of cancer stem cells (CSCs) is considered an essential and major missing piece for better understanding the developmental biology of the disease and designing effective treatments (*4, 5*). Retrospective studies using primary samples from patients with AML led to identification of distinct types of LSCs with immunophenotypes (the specific combinations of surface marker proteins) resembling those of various types of normal hematopoietic stem and progenitor cells (HSPCs) ranging from hematopoietic stem cells (HSCs) ($Lin^-CD34^+CD38^-$) (*6, 7*), to early progenitors ($CD34^+CD38^{-/+}$) such as lymphoid-primed multipotent progenitors (LMPPs), granulocyte-macrophage progenitors (GMPs) (*8*), and more mature ($CD34^-$) GM-precursors (*9, 10*). In contrast, studies aiming to identify pre-LSCs based on detection of candidate driver mutations in "normal" mutated HSPC populations in patients with AML could only infer HSC-like cells as their potential origins (*11, 12*). Although these retrospective approaches using patient samples have provided insights to the origins of human AML stem cells, they have several caveats. Interpretation of these retrospective studies can be complicated by the use of different immunophenotypic definitions for HSPCs in different studies. For example, some studies include the presence of myeloid markers, which are absent in the normal HSPC counterparts, when defining leukemic HSPCs (*8, 9, 11-14*). In addition to immunophenotypes, the function

of the identified pre-leukemic cells or “normal” mutated HSPCs carrying the mutations also differ from their normal counterparts. For example, the pre-leukemic HSC-like cells lack the ability to differentiate into T cells (*11, 12*); which however is a defining and essential property for normal HSCs. An alternative, but not mutually exclusive, approach to retrospective studies is disease modeling using mouse cells. This disease modeling approach has been applied to prospectively identify the potential cellular origins of various cancers including AML (*3-5, 15*).

Given the clinical importance and well-defined genetic features of MLL-rearranged leukemias, prospective functional studies were performed to investigate the potential cells of origin in MLL-AML (*15*). Ectopic expression of MLL-ENL or MLL-GAS7 chimeric fusion in well-defined mouse HSPCs revealed that both HSCs and short-lived myeloid progenitors, including GMPs, serve as the origins of mouse AML stem cells (*16, 17*). Subsequently, ectopic expression of the chimeric transcription factors MLL-AF9 or MOZ-TIF2, both of which are associated with specific genetic variants of human AML, also transforms mouse GMPs (*18-20*), suggesting that HSCs and GMPs are common cellular targets for AML driven by oncogenic chimeric transcription factors. The gene expression profiles of AML originating from mouse GMPs or HSCs also correlate with different prognostic outcomes (*21-24*), suggesting a key function of cells of origin in governing disease biology. However, strong functional evidence for the existence of different origins of immunophenotypically and genetically indistinguishable human AML is lacking. To address the different results obtained from retrospective analyses of human patient samples and prospective disease modeling studies based on mouse cells, reconstruction of the human disease using corresponding human primary cells is key (*25, 26*). Taking advantage of the success in modeling human MLL-AML (*27, 28*) together with the advances in isolating functionally defined human hematopoietic cell populations (*29-31*), the current study identified the potential cells of origin and molecular vulnerability of chemoresistant human MLL-AML stem cells.

Results

Human HSCs and CMPs are cellular targets for MLL-fusion–mediated transformation.

To prospectively and functionally identify the origin of MLL-AML stem cells, we reconstructed human AML cells using highly purified and functionally validated human hematopoietic cells isolated from umbilical cord blood (fig. S1A). The isolated cells including HSCs, CMPs (common myeloid progenitors), LMPPs, and GMPs (fig. S1B-E) were used as as the testing populations in a modified retroviral transduction and transformation assay (RTTA) (*32*), which had been successfully deployed to model human MLL-rearranged leukemia driven by MLL-ENL and MLL-AF9 (*27, 28*).

Since ENL and AF9 are part of the same protein complex (EAP complex, also called AEP complex or SEC, comprised of ENL, AF4, AF9, AF10, ELL, and pTEFb) and their MLL fusions behave similarly in transforming hematopoietic cells in both mouse and human studies (*3*), we used MLL-ENL as a representative MLL-AML involving EAP complexes. We also included the poorly characterized and most common MLL fusion that is not part of EAP complexes, MLL-AF6 (*33*). MLL-AF6 is believed to function by forcing dimerization of truncated MLL (*34, 35*).

Expression of MLL-ENL or MLL-AF6 (collectively referred to as MLLx) in human LMPPs and GMPs had little effect on their growth. Like their normal untransduced counterparts, these cells ceased to proliferate in 3 – 6 weeks (Fig. 1A, fig. S1F). HSCs and CMPs transduced with MLLx continuously proliferated and morphologically resembled immature blasts with myeloid characteristics (Fig. 1A, B). As a quantitative indicator of differentiation status, we used a nitroblue tetrazolium (NBT) assay. Consistent with their immature morphology, few of the HSCs and CMPs transduced with MLLx were NBT-positive (Fig. 1C, figure S2A). Compared to MLLx-transduced LMPPs and GMPs, transduced HSCs and CMPs had lower percentages of apoptotic or necrotic cells (Fig. 1D, fig. S2B) and higher

long-term culture-initiating cell (LTC-IC) frequencies, indicating enhanced self-renewal (Fig. 1E, fig. S2C). Western blot analyses of the HSCs and CMPs transformed by MLLx confirmed their comparable MLL fusion expression as those found in various patient-derived AML cell lines (fig. S2D), demonstrating pathologically relevant amounts of MLL fusion protein in our models despite retroviral expression. Because both MLL-ENL and MLL-AF6 transformed only HSCs and CMPs and not LMPPs and GMPs, this lineage-restricted transformation ability was not unique to MLL fusions that belong to part of the EAP complex.

Despite their different origins, HSCs and CMPs transformed by MLL-ENL or MLL-AF6 exhibited very similar immunophenotypes, $CD34^{-/lo}/CD38^{+}/CD123^{+}/CD45RA^{+/-}/CD11b^{+}/CD13^{+/-}/CD33^{+}/CD45^{+}/CD64^{+}/CD14^{+/-}/CD4^{+}/CD32^{+}/CD15^{+}/HLA\text{-}DR^{+}$ (Fig. 1F), consistent with the biphenotypic immunophenotype of MLL-AML found in patients (*36*) (table S1 in data file S1). This property suggested that human HSCs and CMPs are cells of origin for MLL-AML.

To gain insight into the potential molecular mechanisms underlying differential susceptibility to transformation by MLL fusions, global expression analysis by RNA sequencing (RNA-Seq) was performed at ~14 days after MLL-ENL or MLL-AF6 transduction (table S2 in data file S1). At this time point, all cultures had similar proportions of immature early myeloblasts along with differentiated macrophages (fig. S3A). We combined the results from the cell populations that exhibited transformation (HSC-MLL-ENL, HSC-MLL-AF6, CMP-MLL-ENL, and CMP-MLL-AF6, collectively referred to as HSC/CMP-MLLx) and those that did not (LMPP-MLL-AF6, LMPP-MLL-ENL, GMP-MLL-ENL, and GMP-MLL-AF6, collectively referred to as LMPP/GMP-MLLx). No significant ($p > 0.05$) differences between HSC/CMP-MLLx and LMPP/GMP-MLLx cultures were observed at the level of morphology (fig. S3A) or differentiation (fig. S3B-C).

Principle component analysis of normal and MLLx-transduced cell populations from 2 independent cord blood donors indicated greater variation by cell type than by donor (fig. S3D). Comparable expression of MLL fusion was observed between HSC/CMP-MLLx and LMPP/GMP-MLLx and gene set enrichment analysis (GSEA) revealed activation of MLL-fusion gene expression programs (*37*) in all populations compared to their untransduced counterparts (fig. S3E), indicating functionally and transcriptionally active MLL fusion proteins in all transduced populations. Differential expression analysis (DESeq2) revealed 1295 genes that were significantly (adj. p-value < 0.05) upregulated in MLLx-transduced HSCs or CMPs compared to MLLx-transduced LMPPs or GMPs, and 1780 genes that were downregulated (Fig. 1G, table S3 in data file S1). To focus on genes that show the least variation within each group, a one-way ANOVA was performed [false discovery rate (FDR) < 0.05] on RNAseq read counts that were transformed with two complementary methods (vst – variance stabilizing transformation; and rlog – regularized log transformation from the DESeq2 package) to minimize noise. Their overlap with the differentially expressed genes identified by DESeq2 yielded 45 genes that were highly expressed in HSC/CMP-MLLx (Fig. 1G-H, table S3, 4 in data file S1). Most of the differentially expressed genes, including *MEIS1* and *HMGA2*, were also found in by comparing HSC/CMP-MLLx from late immortalized cultures (6 – 10 weeks) to MLLx-transduced LMPPs and GMPs in short-term culture (fig. S3F, table S3 in data file S1), indicating that these differentially activated genes are critical for transformation of the targeted hematopoietic populations. As a proof-of-principle, two independent shRNAs were employed to knock down *MEIS1* in HSCs or CMPs transduced with MLL-ME to assess its requirement for oncogenic transformation. Compared with scramble controls, MEIS1 knockdown significantly ($p < 0.05$) compromised the LTC-IC activity of HSC or CMP-MLLx, indicating that the 45-gene signature included genes important for transformation of HSCs and CMPs (fig. S3G). Functional annotation using 'webgestalt' revealed the 'acute myeloid

leukemia' transcriptional program as the top associated disease, and 'ToppGene' highlighted 'transcriptional misregulation in cancer' as one of only four pathways associated with the 45-gene signature (Fig. 1H, table S5 in data file S1). Both stem cell and LSC transcriptional programs were highly expressed in HSC/CMP-MLLx (Fig. 1I).

In contrast, we identified 130 differentially upregulated genes in LMPP/GMP-MLLx compared to HSC/CMP-MLLx (Fig. 1G). This 130-gene signature did not have any leukemia association but showed enrichment of the CD family of molecules, many of which are present on differentiating monocytes or macrophages (Fig. 1G, fig. S3H, table S5 in data file S1). Together, these results indicated that despite all transduced populations expressing functional MLL fusion proteins, leukemia and stem cell transcriptional programs essential for transformation were only activated HSCs and CMPs not the branched LMPPs and GMPs, revealing a transformation demarcation between CMPs and LMPPs in MLL-AML.

HSC-MLLx and CMP-MLLx transformed cells induce AML with CSCs in the $CD34^{-/lo}CD38^{+}$ population

To assess their oncogenic potential in vivo, we transplanted HSC-MLLx or CMP-MLLx cells into immunocompromised NSG mice. HSCs or CMPs transformed with MLL-ENL or with MLL-AF6 induced AML with protracted and slightly varying latencies (Fig. 2A). All four populations also produced long-term engraftment and leukemic infiltration into multiple organs (Fig. 2B, fig. S4A-B). Analysis of blood cells in recipients of MLL-AF6 transformed HSCs or CMPs showed white blood cell count, anaemia, and thrombocytopenia (fig. S4C). Given the protracted disease latencies, we evaluated if additional mutations occurred in the cells during disease progression. Whole genome exome sequencing comparing the leukemia cells with early transformed cells was performed on 4 independent pairs of cells (HSC-MLL-ENL, CMP-MLL-ENL, HSC-MLL-AF6, and CMP-MLL-AF6). Relatively few additional genetic changes were identified (fig. S4D, table S2, S6 in data file S1), which is

consistent with low mutational rates identified in MLL-rearranged leukemia patients (*38*). Interestingly. *SFI1*, which encodes a protein involved in spindle assembly, was mutated in both HSC-derived and CMP-derived leukemia samples, suggesting deregulation of the spindle checkpoint as a potential contributing event for disease progression. Immunophenotypically, the HSC-derived and CMP-derived leukemias shared similar and more mature $CD34^{-/lo}CD38^{+}$ phenotypes (fig. S4B, table S1 in data file S1) compared with the originally transduced HSC or CMP populations (fig. S1C).

To demonstrate that functional CSCs were generated in our humanized MLL-rearranged leukemia models, we transplanted primary leukemia cells into secondary recipients. Primary HSC-MLL-AF6 as well as CMP-MLL-AF6 leukemia cells induced leukemia in secondary recipients with similar immunophenotypes (fig. S5A-D), indicating the presence of CSCs in our models. To assess the CSC activity of the transformed cells from the subpopulations of MLLx-transformed HSCs and CMPs, we performed in vitro LTC-IC and in vivo limiting dilution transplantation assays on cells sorted by CD34 and CD38 abundance. A markedly higher LTC-IC frequency was found in $CD34^{-/lo}CD38^{+}$ compartment than in any of the other subpopulations of MLLx-transformed cells derived from either cell of origin (Fig. 2C). Consistent with our in vitro results, in vivo limiting dilution analyses showed that only $CD34^{-/lo}CD38^{+}$ cells propagate in vivo and produce overt leukemia (Fig. 2D, table S7 in data file S1), indicating that AML stem cell activity was highly enriched in the $CD34^{-/lo}CD38^{+}$ compartment. Together, these results support that both HSCs and CMPs are cellular origins of human MLL-AML with CSC activity mostly residing in a phenotypically more mature $CD34^{-/lo}/CD38^{+}$ compartment.

AML stem cell activity is enriched in the $CD34^{-/lo}CD38^{+}$ compartment in patients with MLL-AML

To validate the findings from our humanized models in the clinical settings, we systematically assessed CSC activity in a panel of 16 MLL-AML patient samples, which exhibited variable CD34/CD38 patterns (see details of clinical laboratory findings in table S8 in data file S1). Based on the guidelines by European Group for the Immunological Characterization of Leukemias (EGIL), the patient samples were broadly classified according to their CD34 abundance into a $CD34^{+}$ group (10 patients) with more than 20% $CD34^{+}$ cells, and a $CD34^{-/lo}$ group (6 patients) with less than 20% of cells positive for CD34 (*39*) (fig. S6A, table S1 in data file S1). They were then fractionated based on abundance of CD34 or CD38 and used for in vitro and in vivo functional assays (fig. S6B).

As expected, LTC-IC activity almost exclusively resided in the $CD34^{-/lo}/CD38^{+}$ fraction in the $CD34^{-/lo}$ group (Fig. 3A, fig. S6C). Consistent with the findings in our humanized models, we also observed a significant ($p < 0.05$) enrichment of LTC-IC activity in $CD34^{-/lo}/CD38^{+}$ subpopulation even in the $CD34^{+}$ group (Fig. 3B, fig. S6C). In contrast the $CD34^{-/lo}/CD38^{+}$ cells from cord blood failed to grow in LTC-IC (fig. S6D). Furthermore, cells growing out from the LTC-IC assay contained *MLL* fusions as demonstrated by FISH (fig. S6E), confirming their leukemic origins.

When the subpopulations of cells were assessed in vivo, only the $CD34^{-/lo}CD38^{+}$ cells were capable of inducing AML in vivo (Fig. 3C-D, fig. S7A-C), with an exception of one mouse injected with $CD34^{+}CD38^{-}$ cells from the $CD34^{+}$ group (HMW), which developed leukemia with a remarkably longer latency and lower leukemic burden and tissue infiltration (Fig. 3D, fig. S7A). To quantify the frequency of AML stem cells in each CD34/CD38 fraction, we identified 6 other patient samples (3 for each of the $CD34^{-/lo}$ and $CD34^{+}$ groups) that could engraft into NSG mice and had sufficient material for in vivo limiting dilution assay. AML stem cells in both $CD34^{-/lo}$ and $CD34^{+}$ groups almost exclusively resided in the $CD34^{-/lo}CD38^{+}$ population (ranging from 1 cell in 3,000 to 1 in 277,000) (Fig. 3E-F, table S9 in data file S1).

The only exception was weak CSC activity (1 in 2,300,000) found in the $CD34^+CD38^+$ fraction of patient UPN001; CSC activity of this subpopulation was ~10× lower than that of the $CD34^{-/lo}CD38^+$ subpopulation from the same patient. These data indicated that the $CD34^{-/lo}CD38^+$ fraction of cells as the major source of human MLL-AML stem cells.

We evaluated the CD34/CD38 profiles of the leukemic grafts from mice receiving bulk cells from either patients with samples classified as $CD34^{-/lo}$ or $CD34^+$ and compared the cells to the profiles of the original patient samples. Mice transplanted with bulk cells from $CD34^{-/lo}$ MLL-AML group developed leukemia with similar CD34/38 subpopulations as the original clinical samples (Fig. 3G, fig. S8A). The exception was X25356, which showed an enrichment of $CD34^{-/lo}CD38^+$ cells (Fig. 3G, lower). In contrast, a significant ($p < 0.05$) increase of $CD34^{-/lo}CD38^+$ cells at the expense of the $CD34^+$ population was a common feature in animals of the MLL-AML $CD34^+$ group when compared with their corresponding patient samples (Fig. 3G-H, fig. S8A-S8B). We also evaluated 3 patient cells with non-MLL AML as a control group. The CD34/CD38 profiles of those cells were unchanged from those of the original patient cells when analyzed from leukemic mice (fig. S8A,B). Similar to the data from the bulk unsorted cells, recipients transplanted with purified $CD34^{-/lo}CD38^+$ cells also repopulated $CD34^+$ cells in the hosts (Fig. 3H) and became significantly ($p < 0.05$) enriched in $CD34^{-/lo}CD38^+$ cells compared to their original samples (Fig. 3H, fig. S8C).

To test if the $CD34^{-/lo}CD38^+$ cell population from patients with MLL-AML contain long-term leukemia repopulation capacity, we performed a secondary transplantation of cells from the mice that received primary grafts of $CD34^{-/lo}CD38^+$ cells. Whereas cells from primary engrafted mice that received $CD34^{-/lo}CD38^+$ from either the $CD34^+$ group (HMW and UPN001) or the $CD34^{-/lo}$ group (M519 and X9521) engrafted in secondary recipients (fig. S8D), those from the two rarely engrafted mice transplanted with $CD34^+$ cells ($CD34^+CD38^-$ of HMW in Fig. 3D and $CD34^+CD38^+$ of UPN001 in Fig. 3F) failed to engraft secondary recipients (fig.

S8D). These results indicated that the fully functional CSCs reside in the $CD34^{-/lo}CD38^{+}$ subpopulation. Thus, the $CD34^{-/lo}CD38^{+}$ compartment is the major reservoir for human MLL-AML stem cells.

Human HSC-derived MLL-AML is more resistant to chemotherapy treatment than is CMP-derived MLL-AML

Given the similar immunophenotypes of HSC-derived and CMP-derived human AML, we sought to identify a molecular signature that will predict a potential HSC or CMP origin in AML patients. We performed RNA-seq analyses on human HSC-MLLx and CMP-MLLx leukemia models and their corresponding normal counterparts. Although there were 1,992 differentially expressed genes between normal HSCs and CMPs and 297 between MLLx-transformed HSCs and CMPs, we identified a 23-gene signature that distinguished human HSCs and their derived MLLx-induced leukemia from the CMP counterparts (table S10 in data file S1). To assess the functional relevance of this gene signature in AML patients, we applied a neural network–based machine learning approach (table S11 in data file S1) to stratify 1411 primary human AML samples according to their predicted cell of origin. The 1411 samples were those for which gene expression profiles were publicly available, covering 18 of the 23 genes in the signature and included samples from patients with MLL-AML and other genetic forms of AML. Patients stratified as having AML with an "HSC-like origin" had a significantly shorter median survival ($p < 0.0001$) (Fig. 4A, table S12 in data file S1) compared to patients with AML with a "CMP-like origin". This difference in survival was also present at 1 year and 5 years (fig. S9A). Similar results were obtained when using only the patient subset with MLL-AML (fig. S9B). Moreover, multivariate regression analysis revealed the HSC gene signature as an independent poor prognostic marker (table S13 in data file S1), suggesting that human HSC-like AML has an inferior prognosis and may be more resistant to the current standard chemotherapy treatment than AML of CMP origin.

To establish and experimentally validate the clinical implications of cell of origin in mediating resistance to treatment, we investigated the conventional chemotherapy responses of the humanized models derived from HSCs and CMPs. Compared with MLLx-transformed CMPs, MLLx-transformed HSCs were significantly ($p < 0.01$) less sensitive to cytarabine (Ara-C) and doxorubicin (DOXO) when tested for LTC-IC frequency (Fig. 4B) or chemo-induced differentiation (fig. S10A-B). To confirm the results in vivo, human AML cells derived from either HSCs or CMPs were transplanted into NSG mice, and the mice were administered DOXO chemotherapy treatments. Although DOXO treatment reduced the tumor burden immediately in both HSC-MLL-ENL and CMP-MLL-ENL mice, only HSC-MLL-ENL cells recovered to tumor burden amounts comparable to the untreated control 3 weeks after the treatment (Fig. 4C). This contrasts with the continuous decline of tumor burden in CMP-MLL-ENL mice (Fig. 4C).

To demonstrate the clinical relevance of our findings for patients with AML, we tested primary MLL-AML samples that were stratified into HSC-like or CMP-like AML based on their gene expression signatures (table S14 in data file S1). In line with the results from the humanized leukemia models, HSC-like primary MLL-AML cells were more resistant to conventional chemotherapy treatment than were CMP-like primary MLL-AML cells, which exhibited significantly ($p < 0.05$) lower LTC-IC frequencies (Fig. 4D) and enhanced differentiation (fig. S10C-D) upon exposure to DOXO or Ara-C. Chemotherapy treatment of mice xenografted with primary patient MLL-AML cells consistently revealed that HSC-like AML was refractory to treatment, whereas treatment significantly ($p < 0.05$) extended the survival of recipients of CMP-like leukemia (Fig. 4E, fig. S10E).

We tested the chemoresistance of different CD34/CD38-sorted subpopulations in HSC-like and CMP-like AML patient samples by exposing the sorted cells to DOXO and monitoring LTC-IC frequency. For CMP-like or HSC-like MLL-AML cells, the LSC-enriched $CD34^-$

$^{/lo}$CD38^{+} population was most refractory to DOXO treatment compared to the other populations (fig. S10F, G). However, like the bulk unsorted cells, the CD34$^{-/lo}$CD38^{+} from the CMP-like AML cells were more sensitive to DOXO than CD34$^{-/lo}$CD38^{+} cells from HSC-like AML patient samples (fig. S10H). These data are consistent with the results of the xenograft experiments (Fig. 4D-E). Collectively, these results provide evidence that, although human MLL-AML originating from CMPs responds to chemotherapeutic drugs, HSCs-like MLL-AML is resistant to chemotherapy and needs different treatment.

ABCC3 is a candidate target for chemoresistant HSC-derived MLL-AML

To identify the potential molecular targets responsible for treatment resistance in HSC-derived human MLL-AML, we investigated the 297 differentially expressed genes from the HSC-MLLx versus CMP-MLLx comparison (table S10 in data file S1), and identified 99 genes meeting these criteria: adj.p < 0.05 and log fold change > 1.5 (table S15 in data file S1). By comparison with the Genomic Element Associated with drug Resistance (GEAR) database (*40*), we identified 2 genes associated with DOXO resistance in our set of 99 and in GEAR; one encodes IL6, which was added to the culture medium, and the other encodes ABCC3, a multidrug and organic anion transporter of the ABC family of transporters (Fig. 5A). We confirmed that expression of ABCC3 was higher in HSC-MLLx cells than in CMP-MLLx cells (fig. S11A). In contrast to other ABC family members, relatively little is known about ABCC3 in cancer although its overexpression is implicated in resistance to chemotherapeutic drugs and associates with poor prognosis in both pediatric and adult AML (*41, 42*).

Being an anion organic transporter, ABCC3 may use DOXO as a substrate, we investigated whether high expression of *ABCC3* mediates DOXO resistance in HSC-derived MLL-AML. Knockdown of ABCC3 by two independent shRNAs had only moderate effects on survival of HSC-derived MLL-AML cell lines (Fig. 5B, fig. S11B). However, knocking down ABCC3 significantly ($p < 0.01$) enhanced DOXO sensitivity of HSC-derived MLL-AML

cells, resulting in a dramatic reduction in both cell viability and LTC-IC frequency (Fig. 5B, fig. S11C). To explore the translational potential of this finding, we tested the small molecule inhibitor fidaxomicin, targeting ABCC3, which is currently used for the treatment of diarrhea associated with *Clostridium difficile* infection (*43*). We labelled HSC-MLLx cells with the dye Fluo8-AM, treated the cells with or without fidaxomicin, and monitored dye retention by flow cytometry. Cells treated with fidaxomicin retained significantly ($p < 0.01$) higher amounts of the dye over time, compared to control cells (Fig. 5C). We also observed greater dye retention when ABCC3 was knocked down by either of 2 independent shRNAs (Fig. 5D). Similar to the effect of ABCC3 knockdown (Fig. 5B), combination treatment with fidaxomicin and DOXO significantly ($p = 0.0041$) suppressed LTC-IC frequency and leukemic cell growth of HSC-MLLx cells (Fig. 5E, fig. S11D). Striking results were obtained in vivo using the NSG xenograft model transplanted with HSC-derived MLL-AF6 expressing a luciferase reporter. Whereas treatment with DOXO or fidaxomicin alone had very little effect on cancer burden, their combination significantly ($p<0.001$) reduced tumour burden (Fig. 5F). Together these results revealed an important function and a potential avenue for targeting ABCC3 in chemoresistant HSC-derived MLL-AML.

Fidaxomicin overcomes chemoresistance associated with stem cell origins in primary MLL-AML patient samples

Similar to our humanized cell-of-origin models, samples from patients with HSC-like AML had higher expression of *ABCC3* than samples from patients with CMP-like AML (fig. S12A). To determine the translational potential of targeting ABCC3 in patients with AML, we assessed the ability of fidaxomicin to sensitize primary MLL-AML cells of HSC-like origin to chemotherapy. Whereas primary MLL-AML samples of HSC-like origin consistently showed poor responses to DOXO or fidaxomicin alone, their combination exerted a significant ($p <$

0.05) effect in suppressing leukemic cell growth (Fig. 6A) and LTC-IC frequency (Fig. 6B). The combination also induced differentiation (Fig. 6C, fig. S12B) and apoptosis (Fig. 6D).

To assess the in vivo efficacy of the treatments, HSC-like primary MLL-AML cells from a patient with t(11;17) translocation were transduced with a luciferase reporter prior to their transplantation into NSG mice for monitoring disease kinetics in response to treatment. Compared with the untreated control cohort, fidaxomicin treatment alone did not have any significant ($p = 0.26$) in vivo effect on leukemia cell growth (Fig. 6E, fig. S12C), and recipients developed leukemia with an almost identical latency as the controls (Fig. 6F). Although DOXO alone initially reduced leukemic burden (Fig. 6E, fig. S12C), this monotherapy failed to translate into any significant ($p = 0.2$) survival advantage (Fig. 6F, fig. S12D), suggesting that some of the leukemia cells were sensitive to DOXO but not the treatment-resistant LSCs. Consistent with the in vitro results, fidaxomicin re-sensitized cells to DOXO treatment: The combination suppressed in vivo leukemic cell growth (Fig. 6E, fig. S12C). Importantly, the combination treatment also extended disease-free survival to an extent that none of the recipient hosts succumbed to leukemia during the observation period (Fig. 6F). We confirmed this survival benefit of the combination therapy and reduction in leukemia burden using cells from another patient with HSC-like MLL-AML with t(9;11) translocation (Fig. 6G-H, fig. S12E). Together these results provide the proof-of-principle and pre-clinical data for the use of ABCC3 inhibitor for treatment-resistant MLL-AML stem cells.

Discussion

By combining disease reconstruction using highly purified human HSPCs together with functional deconvolution of AML stem cells from primary patient samples, the current study identified human HSCs and CMPs as two distinctive origins for immunophenotypically indistinguishable $CD34^{-/lo}$ MLL-AML that exhibit contrasting responsiveness to

chemotherapy. While MLL-AML is generally associated with a poor prognosis, there are a large number of high risk patients with AML, including those with MLL-AML, who achieve long-term remission (*2*), suggesting a high degree of heterogeneous treatment responses among patients even those carrying the same driver mutations such that a subset can be cured by current treatments (*44*). Thus, although identification of a chemosensitive subgroup within patients with MLL-AML appears counterintuitive, our findings are consistent with this diversity in patient responsiveness to treatment. Our results are also in line with the findings that chemotherapy can be effective in eradicating certain human LSCs (*45*).

Treatment resistance is thought to be mediated by a subset of cancer cells with specific genetic mutations that confer drug resistance. This resistant population can emerge from pre-existing subclones, or arises during the treatment (*1*). Therapy-resistant cells already present at diagnosis in patients with two major patterns of relapse can originate from rare AML stem cells that have an early HSPC phenotype or from larger subclones of immunophenotypically committed leukemia cells (*14*). Both types of therapy-resistant cells retained transcriptional signatures associated with stemness, which were acquired during transformation (*14*). The current reconstruction and characterization of immunophenotypically indistinguishable human MLL-AML from HSCs and CMPs revealed a critical and additional layer of complexity beyond transforming DNA mutation. Predefined properties of the leukemia cells came from their cell of origin and contributed to the heterogeneity and resistant properties of human AML stem cells. Our study also unveiled the potential of targeting key molecular mediators, such as ABCC3, that are associated with their cell of origin to overcome treatment resistance (fig. S13).

These results in human are different from the previous findings in mouse where GMPs were identified as a major origin of MLL-AML under a similar experimental setting (15-17, 19), suggesting a potential divergence in molecular regulatory networks between human and

mouse GMPs (*29*). Consistently, our findings of distinctive transformation phenotypes exhibited by MLL-AML from HSC (chemoresistant), CMP (chemosensitive), and GMP (non-transformed) origins are in accord with the single cell omics data showing the existence of intrinsic molecular differences among these developmental hierarchical states (*46-49*). These developmental states may play a key role in defining the properties of their transformed counterparts. We discovered that chemoresistant human MLL-AML originating from HSCs has higher *ABCC3* expression, which we found was critical for the resistant property of these cells but was largely dispensable for normal HSC development (*50*). Previous gene expression studies on primary patient samples showed that certain classes of ABC transporters are poor prognostic markers for AML (*41, 42, 51, 52*). Here, we further demonstrated that fidaxomicin, which is currently used for treatment of *Clostridium difficile* infection-associated diarrhea (*43*), is effective in inhibiting ABC transporters and sensitizing LSCs to chemotherapy. This may allow swift translation into the clinical practice for AML treatment.

Historically AML stem cells are thought to mostly be enriched in $CD34^+$ fractions, but emerging evidence indicates their presence in $CD34^-$ fractions (*53*), including those carrying an NPM1c mutation (*9, 10, 54*). Up to now, little was known about the biology and origin of these $CD34^{-/lo}$ AML stem cells. Despite different initiating mutations, both MLL-AML and NPM1c-mutated AML are characterized by aberrant HOX gene expression (*2*). Our recent study reveals that the long noncoding RNA, HOTTIP, which plays a key role in establishment of a chromatin domain for posterior *HOXA* gene expression is required for development of both MLL-AML and NPM1c-mutated AML (*55*), suggesting pathological functions of HOX transcriptional programs in these leukemias. Given aberrant activation of HOX genes as a common feature for a number of AML (*56*) and the requirement of HOX-cofactor, MEIS1 for transformation of HSCs and CMPs, it is tempting to speculate that activation of HOX signaling pathway may be a key determinant for the HSC and CMP origin of $CD34^{-/lo}$ AML stem cells.

Although studies using primary human cells can provide unique insights into human disease biology, they have limitations. Transplantation of human cells in xenografted hosts with different immune barriers and bone marrow niches places a major constraint on the number of cells required for in vivo experiments of human diseases. For example, ~200K cells are required for retroviral transduction and CRISPR models (*27, 57*), and ~1M cells in TALEN models (*58, 59*). The requirement for such large numbers of cells prohibits direct transplantation without ex-vivo expansion. Given the existence of different immunophenotypic definitions of HSPC populations (*29-31, 60*) and our rather limited knowledge about the biochemical differences among different MLL fusions (*3, 15*), the current findings do not exclude the possibility for the existence of other cellular targets, such as $CD34^-$ HSCs (*61*) or differently defined granulocyte myeloid progentiors (*62*), that can be transformed by same MLL fusions studied here or other MLL fusions, such as MLL-AF9 (*63*). Although the use of HSPC populations from cord blood is highly relevant to infant or childhood leukemia where MLL-rearranged leukemia is particularly prevalent, it remains to be determined if the same principles apply to bone marrow HSPCs, which are an alternative source for modeling MLL-AML. Finally, the current study has pinpointed MLL-AML stem cells to $CD34^{-/lo}CD38^+$ fraction, this population however remains highly heterogenous in both our humanized models and patients with MLL-AML. Future in-depth investigations using single cell multi-omics approaches will be important to further refine the identity and molecular functions of human MLL-AML stem cells. While future technological advances and experiments will be instrumental to address some of these outstanding questions, the present study exemplifies the power of combining forward disease modelling with retrospective functional characterization of LSCs using primary human cells to gain unique insights into natural history and biology of human diseases.

Materials and Methods

Study design

The research objective was to functionally reconstruct MLL-AML from different human hematopoitic progenitors to determine potential cells of origin and identity of LSCs and to investigate mechanism of chemoresistance. For disease modelling, cord blood from healthy subjects was transduced with retrovirus carrying MLL fusion gene. Peripheral blood or bone marrow aspirates from AML patients with informed patient consent were obtained from multiple centers. For in vivo experiments, patient MLL-AML cells or MLL fusion-transformed cells were transplanted into NSG mice. Several experimental procedures were carried out, including liquid culture assay, immunophenotyping, apoptosis assay, differentiation assay, LTC-IC assay, methylcellulose culture assay, shRNA knock down, RT-qPCR, Western blotting, RNA-seq, WES, and in vivo transplantation studies. The investigators were not blinded to the sample conditions. Experiments were conducted with multiple samples, trials, or animals (n = 2 – 14). The exact number of n is given in each figure legend. The sample sizes were calculated to demonstrate reproducibility and to achieve statistical significance with a minimum power of 95% (*64*).

Generation of humanized MLL-AML cell lines

A modified retrovirus transduction transformation assay (RTTA)(*32*) was employed for establishment of a model of human cell-of-origin MLL leukemia. Briefly, human cord blood was obtained from Anthony Nolan Cell Therapy Centre and low-density mononuclear cells were isolated using Ficoll according to manufacturer's instructions (GE Healthcare). $CD34^+$ cells were enriched by magnetic activated cell sorting (MACS) separation according to the manufacturer's instructions (Miltenyi Biotech Technology). $CD34^+$ cells were stained with PE-Cy5 labelled lineage antibodies (lin) for 20 mins on ice, washed, and sorted into HSC (lin-

CD34+CD38-CD90+CD45RA-), LMPP (lin-CD34+CD38-CD90-CD45RA+), CMP (lin-CD34+CD38+CD123+CD45RA-), or GMP (lin-CD34+CD38+CD123+CD45RA+) using an ARIA sorter (BD). Post-sort purity of greater than 97% was routinely achieved. Sorted cells were transferred into a 96-well plate and incubated overnight in IMDM (Lonza) +15% fetal bovine serum (FBS) (Sigma) +100ng/ml of each human cytokines SCF, TPO, and FLT3L (Peprotech / Miltenyi). Cells were equally split and infected with retrovirus in the presence of 5 µg/ml polybrene (Sigma) and incubated overnight. The same procedure was repeated on the next day. The following day, cells were transferred to a 48-well plate and cultured in IMDM+15%FBS+20 ng/ml of each human cytokines SCF, TPO, FLT3L, IL3 and IL6 (culturing medium). Fourteen days after the first transduction, cells were counted.

Liquid culture assay

Every week, 400k cells were plated into a new 12-well plate with 2 ml culture medium (IMDM+15%FBS+20 ng/ml human cytokines SCF, TPO, FLT3L, IL3, and IL6). After 3 days incubation, 2 ml cell culture medium was added to the cells bringing the total volume to 4 ml. One week after seeding cells were counted and 400k cells were plated again into a 12-well plate. In vitro culture was continued for up to 15 weeks. In cases where MLL fusion-transformed cell lines were transduced with lentivirus carrying shRNA or luciferase, cells were cultured in the presence of 1 µg/ml puromycin (Invitrogen) for at least 48h or in the presence of 1 mg/ml Hygromycin B (Roche) for at least 96h, respectively.

Patient samples

Primary patient samples were prospectively collected according to the protocols approved and with the informed consent of the patients in multiple centres (King's College Hospital, London, UK; Queen Mary's Hospital, Hong Kong, China; University Hospital, Dresden, Germany;

University Hospital Motol, Prague, Czech). Protocols were approved by IRAS (King's College Hospital), Institutional Review Board of the University of Hong Kong/Hospital Authority Hong Kong West Cluster, IRB (University Hospital, Dresden) and Ethical Committee (University Hospital Motol, Prague). Briefly, the bone marrow or the peripheral blood were collected and subjected to Ficoll isolation according to manufacturer's instructions (GE Healthcare). Low-density mononuclear cells were isolated and frozen at -80°C in PBS containing 10% DMSO + 10% FBS using Nalgene Mr.Frosty. Cells were then transferred to liquid nitrogen the next day for long-term storage. Patient information and their clinical characteristics are summarized in table S8.

Constructs

The following MLL fusions were used in this study: MLL-AF6 (MSCVneo or MIGR), consisting of aa35-347 of the AF6 portion (*65*) and MLL-ENL (MSCVblast (*24*) or MIGR). Lentiviral plasmids (pLKO.1-puro) encoding shRNA targeting ABCC3 [TRCN0000059403, TRCN0000059406] and MEIS1 [TRCN0000015971, TRCN0000015972] were obtained from Dharmacon. Luciferase expressing lentivirus pCDH-CMV-luc-EF1-Hygro has been described (*66, 67*). Virus packaging was performed as described (*32*).

In vivo xenotransplantation

All experimental procedures were approved by King's College London ethics committees and conform to the UK Home Office regulations. For all in vivo experiments, mice were distributed into their respective groups randomly. Investigators were not blinded to the sample identity. For human MLL-fusion cord blood model, 1 million MLL-fusion in vitro transformed HSC or CMP populations were transplanted through the intra-femoral route into 6 – 12 week old sub-lethally irradiated (250 cGy) NOD.Cg-Prkdcscid Il2rgtm1Wjl/SzJ (NSG mice; The Jackson

Laboratory Stock No:005557). Some cells were labelled with luciferase reporter and the tumor burden was monitored and quantified using an IVIS Lumina II (Perkin Elmer) as previously reported (*67*). Briefly, cells were tagged with a lentiviral luciferase reporter. Transplanted mice were injected with 150 mg/kg of D-luciferin intraperitoneally 10 mins before bioluminescence image was acquired using IVIS Lumina II (Caliper; Perkin Elmer) and the radiance was measured with software Living Image Version 4.3.1 according to the manufacturer's instructions. For primary patient samples, cells were transplanted into sublethally irradiated (250 cGy) NSG mice via intra-femoral route. For experiments that assessed leukemia burden pre- and post-drug treatment by bone marrow aspiration, cells were transplanted intra-venously (i.v.). In vivo limiting dilution assays were performed with varying cell doses. At least 2 animals received cells at any given dose in most cases. The LTC-IC frequency was determined using online resources - WEHI Extreme Limiting Dilution Analysis (http://bioinf.wehi.edu.au/software/elda/). For transplantation of sorted CD34/CD38 fractions from the human MLL-fusion cord blood model as well as primary patient samples, sorted cells were transplanted in different cell doses for in vivo limiting dilution analysis and 200K cells for each fraction for analysis of disease-free survival.

Analysis of mouse models

When animals showed signs of sickness, such as shortness of breath, hunched posture, lethargy, or weight loss, the mice were euthanized in a CO_2 chamber and confirmed dead by cervical dislocation. Cells mechanically dissociated from tissues, such as flushing out bone marrow cells or grinding spleen and liver tissues on a 45-µm cell strainer (Greiner), were subjected to FACS or flow cytometry analysis. Part of the spleen and liver were fixed in formalin solution and subjected to section and H&E staining. The composition of peripheral blood was analysed by Mythic 18 haematology analyser (Orphee). Blood smears were stained with May-Grunwald-

Giemsa (Sigma). Human AML engraftment is defined by cells positive for both CD45 and CD33. The leukemic mouse is defined by >20% human AML engraftment in the bone marrow with or without tumour infiltration into spleen or liver. The threshold of human AML engraftment for in vivo limiting dilution analysis is set to 1% in the bone marrow of the recipient animals.

In vivo drug treatment

Two weeks after transplantation 0.75 mg/kg DOXO was administered intravenously (i.v.) for 3 days. In some experiments, mice also received 75 mg/kg fidaxomicin i.v. for 3 days. Bioimaging was performed using IVIS Lumina II (Perkin Elmer) as described under "in vivo xenotransplantation".

LTC-IC assay

Human MLL-fusion transduced cord blood cells or primary MLL-AML primary samples (Bulk or CD34/CD38 sorted) were seeded into 96-well plates with MS5 stroma cells in 200 µl medium (IMDM + 15% FBS + 20 ng/mL of each human cytokines IL-3, IL-6, TPO, SCF, and FLT3 ligand). Different cell doses were seeded for 10 or 20 wells per cell dose.

For the LTC-IC assay with drug treatment, cells were either vehicle treated or treated with 100 nM Ara-C, 10 nM doxorubicin, with or without 5 µM fidaxomicin for one week. After one week, all media were replenished with fresh media without drugs and further cultured for other two weeks with media replenished every week. Cell clusters (cobblestone) were scored from each well and the initiating frequency was calculated using online resources - WEHI Extreme Limiting Dilution Analysis (http://bioinf.wehi.edu.au/software/elda/).

RNA-sequencing

50-100 ng (RNAeasy micro, Qiagen) or 300-1000 ng (mirVANA, Ambion) of isolated total RNA was used for RNA-Seq library preparation using TruSeq Stranded Total RNA kit (Illumina) and sequenced on HIseq2000 platform (Illumina) as per manufacturer's recommendations. All samples are listed in table S2 in data file S1.

Human whole exome sequencing assay

Initial human WES was carried out to identify candidate somatic mutations in the exomes of genes. Genomic DNA was isolated from MLLx in vitro transformed cell populations (at 4-8 weeks in culture) and their corresponding leukemic counterparts (i.e. transplanted MLLx in vitro transformed cell populations which induced disease in NSG mice and were harvested from these leukemic mice). Genomic exome library was captured and constructed according to SureSelect Human All Exon V6 kit (Agilent), and these libraries were sequenced using an Illumina 150 bp paired-end sequencing platform. Detail on bioinformatics analysis is in the supplementary materials and methods.

Quantification and statistical analysis

All statistical tests are mentioned in the respective figure legend or main text. Groups that were statistically compared shared a similar variance and all error bars represent SD. The disease-free survival comparisons were performed by Log-rank test in Prism (GraphPad). P-value < 0.05 is considered statistically significant. The number of samples, trials, or animals (n) are indicated in each respective figure legend.

Supplementary Materials

Materials and methods

Data file S1. Tables S1-S15

Table S1 Immunotype of primary MLL-fusion cell lines, cells from the recipient animals and primary patient samples

Table S2 List of samples used for bioinformatic analysis

Table S3 Differential gene analysis by DeSeq2 and one-way ANOVA test after Rlog and Vst transformation

Table S4 List of genes differentially upregulated in HSC/CMP (45 genes) and LMPP/GMP (130 genes)

Table S5 Functional annotation by Toppgene and Webgestalt (2013 version)

Table S6 Acquired SNVs in leukemic samples

Table S7 In vivo limiting dilution analysis of cord blood-derived MLL-AF6; cell dose and response

Table S8 Patient clinical particular

Table S9 In vivo limiting dilution analysis of primary patient samples; cell dose and response

Table S10 Signal genes used in neural network

Table S11 Neural network training and test sets Table S12 Neural network classification for patients in microarray sets

Table S13 Multi-variate analysis of variables affecting overall survival

Table S14 Neural network classification for MLL-fusion patients
Table S15 99 genes differentially expressed in transformed HSC-MLLx vs CMP-MLLx

Data file S2. Raw data for main text Figures 1 – 6

Data file S3. Raw data for supplementary figures S1 – S12

References and notes

1. A. Kreso, J. E. Dick, Evolution of the cancer stem cell model. *Cell Stem Cell* **14**, 275-291 (2014); published online EpubMar 6 (10.1016/j.stem.2014.02.006).
2. B. B. Zeisig, A. G. Kulasekararaj, G. J. Mufti, C. W. So, SnapShot: Acute myeloid leukemia. *Cancer Cell* **22**, 698-698 e691 (2012); published online EpubNov 13 (10.1016/j.ccr.2012.10.017 S1535-6108(12)00445-X [pii]).
3. B. B. Zeisig, C. W. So, in *Chromosomal Translocations and Genome Rearrangements in Cancer,* J. D. Rowley, M. M. Le Beau, T. H. Rabbitts, Eds. (Springer, USA, 2016), chap. 11, pp. 223-250.
4. C. Blanpain, Tracing the cellular origin of cancer. *Nat Cell Biol* **15**, 126-134 (2013); published online EpubFeb (10.1038/ncb2657).
5. J. E. Visvader, Cells of origin in cancer. *Nature* **469**, 314-322 (2011); published online EpubJan 20 (10.1038/nature09781).
6. T. Lapidot, C. Sirard, J. Vormoor, B. Murdoch, T. Hoang, J. Caceres-Cortes, M. Minden, B. Paterson, M. A. Caligiuri, J. E. Dick, A cell initiating human acute myeloid leukaemia after transplantation into SCID mice. *Nature* **367**, 645-648 (1994)10.1038/367645a0).
7. D. Bonnet, J. E. Dick, Human acute myeloid leukemia is organized as a hierarchy that originates from a primitive hematopoietic cell. *Nat Med* **3**, 730-737 (1997); published online EpubJul (
8. N. Goardon, E. Marchi, A. Atzberger, L. Quek, A. Schuh, S. Soneji, P. Woll, A. Mead, K. A. Alford, R. Rout, S. Chaudhury, A. Gilkes, S. Knapper, K. Beldjord, S. Begum, S. Rose, N. Geddes, M. Griffiths, G. Standen, A. Sternberg, J. Cavenagh, H. Hunter, D. Bowen, S. Killick, L. Robinson, A. Price, E. Macintyre, P. Virgo, A. Burnett, C. Craddock, T. Enver, S. E. Jacobsen, C. Porcher, P. Vyas, Coexistence of LMPP-like and GMP-like leukemia stem cells in acute myeloid leukemia. *Cancer Cell* **19**, 138-152 (2011); published online EpubJan 18 (
9. L. Quek, G. W. Otto, C. Garnett, L. Lhermitte, D. Karamitros, B. Stoilova, I. J. Lau, J. Doondeea, B. Usukhbayar, A. Kennedy, M. Metzner, N. Goardon, A. Ivey, C. Allen, R. Gale, B. Davies, A. Sternberg, S. Killick, H. Hunter, P. Cahalin, A. Price, A. Carr, M. Griffiths, P. Virgo, S. Mackinnon, D. Grimwade, S. Freeman, N. Russell, C. Craddock, A. Mead, A. Peniket, C. Porcher, P. Vyas, Genetically distinct leukemic stem cells in human CD34- acute myeloid leukemia are arrested at a hemopoietic precursor-like stage. *J Exp Med* **213**, 1513-1535 (2016); published online EpubJul 25 (10.1084/jem.20151775).
10. D. C. Taussig, J. Vargaftig, F. Miraki-Moud, E. Griessinger, K. Sharrock, T. Luke, D. Lillington, H. Oakervee, J. Cavenagh, S. G. Agrawal, T. A. Lister, J. G. Gribben, D. Bonnet, Leukemia-initiating cells from some acute myeloid leukemia patients with mutated nucleophosmin reside in the CD34(-) fraction. *Blood* **115**, 1976-1984 (2010); published online EpubMar 11 (10.1182/blood-2009-02-206565).
11. L. I. Shlush, S. Zandi, A. Mitchell, W. C. Chen, J. M. Brandwein, V. Gupta, J. A. Kennedy, A. D. Schimmer, A. C. Schuh, K. W. Yee, J. L. McLeod, M. Doedens, J. J. Medeiros, R. Marke, H. J. Kim, K. Lee, J. D. McPherson, T. J. Hudson, H. P.-L. G. P. Consortium, A. M. Brown, F. Yousif, Q. M. Trinh, L. D. Stein, M. D. Minden, J. C. Wang, J. E. Dick, Identification of pre-leukaemic haematopoietic stem cells in acute leukaemia. *Nature* **506**, 328-333 (2014); published online EpubFeb 20 (10.1038/nature13038).
12. M. Jan, T. M. Snyder, M. R. Corces-Zimmerman, P. Vyas, I. L. Weissman, S. R. Quake, R. Majeti, Clonal evolution of preleukemic hematopoietic stem cells precedes human acute myeloid leukemia. *Sci Transl Med* **4**, 149ra118 (2012); published online EpubAug 29 (10.1126/scitranslmed.3004315).
13. M. Jan, M. P. Chao, A. C. Cha, A. A. Alizadeh, A. J. Gentles, I. L. Weissman, R. Majeti, Prospective separation of normal and leukemic stem cells based on differential expression of TIM3, a human acute myeloid leukemia stem cell marker. *Proc Natl Acad Sci U S A* **108**, 5009-5014 (2011); published online EpubMar 22 (10.1073/pnas.1100551108).
14. L. I. Shlush, A. Mitchell, L. Heisler, S. Abelson, S. W. K. Ng, A. Trotman-Grant, J. J. F. Medeiros, A. Rao-Bhatia, I. Jaciw-Zurakowsky, R. Marke, J. L. McLeod, M. Doedens, G. Bader, V. Voisin,

C. Xu, J. D. McPherson, T. J. Hudson, J. C. Y. Wang, M. D. Minden, J. E. Dick, Tracing the origins of relapse in acute myeloid leukaemia to stem cells. *Nature* **547**, 104-108 (2017); published online EpubJul 6 (10.1038/nature22993).

15. A. V. Krivtsov, S. A. Armstrong, MLL translocations, histone modifications and leukaemia stem-cell development. *Nat Rev Cancer* **7**, 823-833 (2007); published online EpubNov (
16. A. Cozzio, E. Passegue, P. M. Ayton, H. Karsunky, M. L. Cleary, I. L. Weissman, Similar MLL-associated leukemias arising from self-renewing stem cells and short-lived myeloid progenitors. *Genes Dev* **17**, 3029-3035 (2003); published online EpubDec 15 (
17. C. W. So, H. Karsunky, E. Passegue, A. Cozzio, I. L. Weissman, M. L. Cleary, MLL-GAS7 transforms multipotent hematopoietic progenitors and induces mixed lineage leukemias in mice. *Cancer Cell* **3**, 161-171 (2003); published online EpubFeb (
18. B. J. Huntly, H. Shigematsu, K. Deguchi, B. H. Lee, S. Mizuno, N. Duclos, R. Rowan, S. Amaral, D. Curley, I. R. Williams, K. Akashi, D. G. Gilliland, MOZ-TIF2, but not BCR-ABL, confers properties of leukemic stem cells to committed murine hematopoietic progenitors. *Cancer Cell* **6**, 587-596 (2004); published online EpubDec (
19. A. V. Krivtsov, D. Twomey, Z. Feng, M. C. Stubbs, Y. Wang, J. Faber, J. E. Levine, J. Wang, W. C. Hahn, D. G. Gilliland, T. R. Golub, S. A. Armstrong, Transformation from committed progenitor to leukaemia stem cell initiated by MLL-AF9. *Nature* **442**, 818-822 (2006); published online EpubAug 17 (
20. T. C. Somervaille, C. J. Matheny, G. J. Spencer, M. Iwasaki, J. L. Rinn, D. M. Witten, H. Y. Chang, S. A. Shurtleff, J. R. Downing, M. L. Cleary, Hierarchical maintenance of MLL myeloid leukemia stem cells employs a transcriptional program shared with embryonic rather than adult stem cells. *Cell Stem Cell* **4**, 129-140 (2009); published online EpubFeb 6 (
21. A. V. Krivtsov, M. E. Figueroa, A. U. Sinha, M. C. Stubbs, Z. Feng, P. J. Valk, R. Delwel, K. Dohner, L. Bullinger, A. L. Kung, A. M. Melnick, S. A. Armstrong, Cell of origin determines clinically relevant subtypes of MLL-rearranged AML. *Leukemia* **27**, 852-860 (2013); published online EpubApr (10.1038/leu.2012.363).
22. J. George, A. Uyar, K. Young, L. Kuffler, K. Waldron-Francis, E. Marquez, D. Ucar, J. J. Trowbridge, Leukaemia cell of origin identified by chromatin landscape of bulk tumour cells. *Nat Commun* **7**, 12166 (2016)10.1038/ncomms12166).
23. V. Stavropoulou, S. Kaspar, L. Brault, M. A. Sanders, S. Juge, S. Morettini, A. Tzankov, M. Iacovino, I. J. Lau, T. A. Milne, H. Royo, M. Kyba, P. J. Valk, A. H. Peters, J. Schwaller, MLL-AF9 Expression in Hematopoietic Stem Cells Drives a Highly Invasive AML Expressing EMT-Related Genes Linked to Poor Outcome. *Cancer Cell* **30**, 43-58 (2016); published online EpubJul 11 (10.1016/j.ccell.2016.05.011).
24. T. Siriboonpiputtana, B. B. Zeisig, M. Zarowiecki, T. K. Fung, M. Mallardo, C. T. Tsai, P. N. I. Lau, Q. C. Hoang, P. Veiga, J. Barnes, C. Lynn, A. Wilson, B. Lenhard, C. W. E. So, Transcriptional memory of cells of origin overrides beta-catenin requirement of MLL cancer stem cells. *EMBO J* **36**, 3139-3155 (2017); published online EpubNov 2 (10.15252/embj.201797994).
25. P. A. Beer, C. J. Eaves, Modeling Normal and Disordered Human Hematopoiesis. *Trends Cancer* **1**, 199-210 (2015); published online EpubNov (10.1016/j.trecan.2015.09.002).
26. S. Balani, L. V. Nguyen, C. J. Eaves, Modeling the process of human tumorigenesis. *Nat Commun* **8**, 15422 (2017); published online EpubMay 25 (10.1038/ncomms15422).
27. F. Barabe, J. A. Kennedy, K. J. Hope, J. E. Dick, Modeling the initiation and progression of human acute leukemia in mice. *Science* **316**, 600-604 (2007); published online EpubApr 27 (
28. J. Wei, M. Wunderlich, C. Fox, S. Alvarez, J. C. Cigudosa, J. S. Wilhelm, Y. Zheng, J. A. Cancelas, Y. Gu, M. Jansen, J. F. Dimartino, J. C. Mulloy, Microenvironment determines lineage fate in a human model of MLL-AF9 leukemia. *Cancer Cell* **13**, 483-495 (2008); published online EpubJun (
29. S. Doulatov, F. Notta, E. Laurenti, J. E. Dick, Hematopoiesis: a human perspective. *Cell Stem Cell* **10**, 120-136 (2012); published online EpubFeb 3 (10.1016/j.stem.2012.01.006).

30. M. G. Manz, T. Miyamoto, K. Akashi, I. L. Weissman, Prospective isolation of human clonogenic common myeloid progenitors. *Proc Natl Acad Sci U S A* **99**, 11872-11877 (2002); published online EpubSep 3 (10.1073/pnas.172384399).
31. C. Y. Park, R. Majeti, I. L. Weissman, In vivo evaluation of human hematopoiesis through xenotransplantation of purified hematopoietic stem cells from umbilical cord blood. *Nat Protoc* **3**, 1932-1940 (2008)10.1038/nprot.2008.194).
32. B. B. Zeisig, C. W. So, Retroviral/Lentiviral transduction and transformation assay. *Methods Mol Biol* **538**, 207-229 (2009)10.1007/978-1-59745-418-6_10).
33. C. Meyer, T. Burmeister, D. Groger, G. Tsaur, L. Fechina, A. Renneville, R. Sutton, N. C. Venn, M. Emerenciano, M. S. Pombo-de-Oliveira, C. Barbieri Blunck, B. Almeida Lopes, J. Zuna, J. Trka, P. Ballerini, H. Lapillonne, M. De Braekeleer, G. Cazzaniga, L. Corral Abascal, V. H. J. van der Velden, E. Delabesse, T. S. Park, S. H. Oh, M. L. M. Silva, T. Lund-Aho, V. Juvonen, A. S. Moore, O. Heidenreich, J. Vormoor, E. Zerkalenkova, Y. Olshanskaya, C. Bueno, P. Menendez, A. Teigler-Schlegel, U. Zur Stadt, J. Lentes, G. Gohring, A. Kustanovich, O. Aleinikova, B. W. Schafer, S. Kubetzko, H. O. Madsen, B. Gruhn, X. Duarte, P. Gameiro, E. Lippert, A. Bidet, J. M. Cayuela, E. Clappier, C. N. Alonso, C. M. Zwaan, M. M. van den Heuvel-Eibrink, S. Izraeli, L. Trakhtenbrot, P. Archer, J. Hancock, A. Moricke, J. Alten, M. Schrappe, M. Stanulla, S. Strehl, A. Attarbaschi, M. Dworzak, O. A. Haas, R. Panzer-Grumayer, L. Sedek, T. Szczepanski, A. Caye, L. Suarez, H. Cave, R. Marschalek, The MLL recombinome of acute leukemias in 2017. *Leukemia* **32**, 273-284 (2018); published online EpubFeb (10.1038/leu.2017.213).
34. C. W. So, M. Lin, P. M. Ayton, E. H. Chen, M. L. Cleary, Dimerization contributes to oncogenic activation of MLL chimeras in acute leukemias. *Cancer Cell* **4**, 99-110 (2003); published online EpubAug (
35. M. E. Martin, T. A. Milne, S. Bloyer, K. Galoian, W. Shen, D. Gibbs, H. W. Brock, R. Slany, J. L. Hess, Dimerization of MLL fusion proteins immortalizes hematopoietic cells. *Cancer Cell* **4**, 197-207 (2003); published online EpubSep (
36. M. R. Baer, C. C. Stewart, D. Lawrence, D. C. Arthur, K. Mrozek, M. P. Strout, F. R. Davey, C. A. Schiffer, C. D. Bloomfield, Acute myeloid leukemia with 11q23 translocations: myelomonocytic immunophenotype by multiparameter flow cytometry. *Leukemia* **12**, 317-325 (1998); published online EpubMar (
37. M. E. Ross, R. Mahfouz, M. Onciu, H. C. Liu, X. Zhou, G. Song, S. A. Shurtleff, S. Pounds, C. Cheng, J. Ma, R. C. Ribeiro, J. E. Rubnitz, K. Girtman, W. K. Williams, S. C. Raimondi, D. C. Liang, L. Y. Shih, C. H. Pui, J. R. Downing, Gene expression profiling of pediatric acute myelogenous leukemia. *Blood* **104**, 3679-3687 (2004); published online EpubDec 01 (10.1182/blood-2004-03-1154).
38. A. K. Andersson, J. Ma, J. Wang, X. Chen, A. L. Gedman, J. Dang, J. Nakitandwe, L. Holmfeldt, M. Parker, J. Easton, R. Huether, R. Kriwacki, M. Rusch, G. Wu, Y. Li, H. Mulder, S. Raimondi, S. Pounds, G. Kang, L. Shi, J. Becksfort, P. Gupta, D. Payne-Turner, B. Vadodaria, K. Boggs, D. Yergeau, J. Manne, G. Song, M. Edmonson, P. Nagahawatte, L. Wei, C. Cheng, D. Pei, R. Sutton, N. C. Venn, A. Chetcuti, A. Rush, D. Catchpoole, J. Heldrup, T. Fioretos, C. Lu, L. Ding, C. H. Pui, S. Shurtleff, C. G. Mullighan, E. R. Mardis, R. K. Wilson, T. A. Gruber, J. Zhang, J. R. Downing, P. St. Jude Children's Research Hospital-Washington University Pediatric Cancer Genome, The landscape of somatic mutations in infant MLL-rearranged acute lymphoblastic leukemias. *Nat Genet* **47**, 330-337 (2015); published online EpubApr (10.1038/ng.3230).
39. M. C. Bene, G. Castoldi, W. Knapp, W. D. Ludwig, E. Matutes, A. Orfao, M. B. van't Veer, Proposals for the immunological classification of acute leukemias. European Group for the Immunological Characterization of Leukemias (EGIL). *Leukemia* **9**, 1783-1786 (1995); published online EpubOct (
40. Y. Y. Wang, W. H. Chen, P. P. Xiao, W. B. Xie, Q. Luo, P. Bork, X. M. Zhao, GEAR: A database of Genomic Elements Associated with drug Resistance. *Sci Rep* **7**, 44085 (2017); published online EpubMar 15 (10.1038/srep44085).

41. Z. Benderra, A. M. Faussat, L. Sayada, J. Y. Perrot, R. Tang, D. Chaoui, H. Morjani, C. Marzac, J. P. Marie, O. Legrand, MRP3, BCRP, and P-glycoprotein activities are prognostic factors in adult acute myeloid leukemia. *Clin Cancer Res* **11**, 7764-7772 (2005); published online EpubNov 1 (10.1158/1078-0432.CCR-04-1895).
42. D. Steinbach, J. Lengemann, A. Voigt, J. Hermann, F. Zintl, A. Sauerbrey, Response to chemotherapy and expression of the genes encoding the multidrug resistance-associated proteins MRP2, MRP3, MRP4, MRP5, and SMRP in childhood acute myeloid leukemia. *Clin Cancer Res* **9**, 1083-1086 (2003); published online EpubMar (
43. Y. Golan, L. Epstein, Safety and efficacy of fidaxomicin in the treatment of Clostridium difficile-associated diarrhea. *Therap Adv Gastroenterol* **5**, 395-402 (2012); published online EpubNov (10.1177/1756283X12461294).
44. D. Grimwade, R. K. Hills, A. V. Moorman, H. Walker, S. Chatters, A. H. Goldstone, K. Wheatley, C. J. Harrison, A. K. Burnett, Refinement of cytogenetic classification in acute myeloid leukemia: determination of prognostic significance of rare recurring chromosomal abnormalities among 5876 younger adult patients treated in the United Kingdom Medical Research Council trials. *Blood* **116**, 354-365 (2010); published online EpubJul 22 (blood-2009-11-254441 [pii]
10.1182/blood-2009-11-254441).
45. A. L. Boyd, L. Aslostovar, J. Reid, W. Ye, B. Tanasijevic, D. P. Porras, Z. Shapovalova, M. Almakadi, R. Foley, B. Leber, A. Xenocostas, M. Bhatia, Identification of Chemotherapy-Induced Leukemic-Regenerating Cells Reveals a Transient Vulnerability of Human AML Recurrence. *Cancer Cell* **34**, 483-498 e485 (2018); published online EpubSep 10 (10.1016/j.ccell.2018.08.007).
46. J. D. Buenrostro, M. R. Corces, C. A. Lareau, B. Wu, A. N. Schep, M. J. Aryee, R. Majeti, H. Y. Chang, W. J. Greenleaf, Integrated Single-Cell Analysis Maps the Continuous Regulatory Landscape of Human Hematopoietic Differentiation. *Cell* **173**, 1535-1548 e1516 (2018); published online EpubMay 31 (10.1016/j.cell.2018.03.074).
47. D. Pellin, M. Loperfido, C. Baricordi, S. L. Wolock, A. Montepeloso, O. K. Weinberg, A. Biffi, A. M. Klein, L. Biasco, A comprehensive single cell transcriptional landscape of human hematopoietic progenitors. *Nat Commun* **10**, 2395 (2019); published online EpubJun 3 (10.1038/s41467-019-10291-0).
48. L. Velten, S. F. Haas, S. Raffel, S. Blaszkiewicz, S. Islam, B. P. Hennig, C. Hirche, C. Lutz, E. C. Buss, D. Nowak, T. Boch, W. K. Hofmann, A. D. Ho, W. Huber, A. Trumpp, M. A. Essers, L. M. Steinmetz, Human haematopoietic stem cell lineage commitment is a continuous process. *Nat Cell Biol* **19**, 271-281 (2017); published online EpubApr (10.1038/ncb3493).
49. S. Zheng, E. Papalexi, A. Butler, W. Stephenson, R. Satija, Molecular transitions in early progenitors during human cord blood hematopoiesis. *Mol Syst Biol* **14**, e8041 (2018); published online EpubMar 15 (10.15252/msb.20178041).
50. M. G. Belinsky, P. A. Dawson, I. Shchaveleva, L. J. Bain, R. Wang, V. Ling, Z. S. Chen, A. Grinberg, H. Westphal, A. Klein-Szanto, A. Lerro, G. D. Kruh, Analysis of the in vivo functions of Mrp3. *Mol Pharmacol* **68**, 160-168 (2005); published online EpubJul (10.1124/mol.104.010587).
51. B. Chapuy, R. Koch, U. Radunski, S. Corsham, N. Cheong, N. Inagaki, N. Ban, D. Wenzel, D. Reinhardt, A. Zapf, S. Schweyer, F. Kosari, W. Klapper, L. Truemper, G. G. Wulf, Intracellular ABC transporter A3 confers multidrug resistance in leukemia cells by lysosomal drug sequestration. *Leukemia* **22**, 1576-1586 (2008); published online EpubAug (10.1038/leu.2008.103).
52. D. Damiani, M. Tiribelli, E. Calistri, A. Geromin, A. Chiarvesio, A. Michelutti, M. Cavallin, R. Fanin, The prognostic value of P-glycoprotein (ABCB) and breast cancer resistance protein (ABCG2) in adults with de novo acute myeloid leukemia with normal karyotype. *Haematologica* **91**, 825-828 (2006); published online EpubJun (

53. K. Eppert, K. Takenaka, E. R. Lechman, L. Waldron, B. Nilsson, P. van Galen, K. H. Metzeler, A. Poeppl, V. Ling, J. Beyene, A. J. Canty, J. S. Danska, S. K. Bohlander, C. Buske, M. D. Minden, T. R. Golub, I. Jurisica, B. L. Ebert, J. E. Dick, Stem cell gene expression programs influence clinical outcome in human leukemia. *Nat Med* **17**, 1086-1093 (2011); published online EpubSep (
54. M. P. Martelli, V. Pettirossi, C. Thiede, E. Bonifacio, F. Mezzasoma, D. Cecchini, R. Pacini, A. Tabarrini, R. Ciurnelli, I. Gionfriddo, N. Manes, R. Rossi, L. Giunchi, U. Oelschlagel, L. Brunetti, M. Gemei, M. Delia, G. Specchia, A. Liso, M. Di Ianni, F. Di Raimondo, F. Falzetti, L. Del Vecchio, M. F. Martelli, B. Falini, CD34+ cells from AML with mutated NPM1 harbor cytoplasmic mutated nucleophosmin and generate leukemia in immunocompromised mice. *Blood* **116**, 3907-3922 (2010); published online EpubNov 11 (10.1182/blood-2009-08-238899).
55. H. Luo, G. Zhu, J. Xu, Q. Lai, B. Yan, Y. Guo, T. K. Fung, B. B. Zeisig, Y. Cui, J. Zha, C. Cogle, F. Wang, B. Xu, F. C. Yang, W. Li, C. W. E. So, Y. Qiu, M. Xu, S. Huang, HOTTIP lncRNA Promotes Hematopoietic Stem Cell Self-Renewal Leading to AML-like Disease in Mice. *Cancer Cell* **36**, 645-659 e648 (2019); published online EpubDec 9 (10.1016/j.ccell.2019.10.011).
56. N. Cheung, C. W. So, Transcriptional and epigenetic networks in haematological malignancy. *FEBS Lett* **585**, 2100-2111 (2011); published online EpubJul 7 (
57. J. Jeong, A. Jager, P. Domizi, M. Pavel-Dinu, L. Gojenola, M. Iwasaki, M. C. Wei, F. Pan, J. L. Zehnder, M. H. Porteus, K. L. Davis, M. L. Cleary, High-efficiency CRISPR induction of t(9;11) chromosomal translocations and acute leukemias in human blood stem cells. *Blood Adv* **3**, 2825-2835 (2019); published online EpubOct 8 (10.1182/bloodadvances.2019000450).
58. C. Buechele, E. H. Breese, D. Schneidawind, C. H. Lin, J. Jeong, J. Duque-Afonso, S. H. Wong, K. S. Smith, R. S. Negrin, M. Porteus, M. L. Cleary, MLL leukemia induction by genome editing of human CD34+ hematopoietic cells. *Blood* **126**, 1683-1694 (2015); published online EpubOct 1 (10.1182/blood-2015-05-646398).
59. C. Schneidawind, J. Jeong, D. Schneidawind, I. S. Kim, J. Duque-Afonso, S. H. K. Wong, M. Iwasaki, E. H. Breese, J. L. Zehnder, M. Porteus, M. L. Cleary, MLL leukemia induction by t(9;11) chromosomal translocation in human hematopoietic stem cells using genome editing. *Blood Adv* **2**, 832-845 (2018); published online EpubApr 24 (10.1182/bloodadvances.2017013748).
60. S. Haas, A. Trumpp, M. D. Milsom, Causes and Consequences of Hematopoietic Stem Cell Heterogeneity. *Cell Stem Cell* **22**, 627-638 (2018); published online EpubMay 3 (10.1016/j.stem.2018.04.003).
61. F. Anjos-Afonso, E. Currie, H. G. Palmer, K. E. Foster, D. C. Taussig, D. Bonnet, CD34(-) cells at the apex of the human hematopoietic stem cell hierarchy have distinctive cellular and molecular signatures. *Cell Stem Cell* **13**, 161-174 (2013); published online EpubAug 1 (10.1016/j.stem.2013.05.025).
62. L. Edvardsson, J. Dykes, T. Olofsson, Isolation and characterization of human myeloid progenitor populations--TpoR as discriminator between common myeloid and megakaryocyte/erythroid progenitors. *Exp Hematol* **34**, 599-609 (2006); published online EpubMay (10.1016/j.exphem.2006.01.017).
63. S. F. Cai, S. H. Chu, A. D. Goldberg, S. Parvin, R. P. Koche, J. L. Glass, E. M. Stein, M. S. Tallman, F. Sen, C. A. Famulare, M. Cusan, C. H. Huang, C. W. Chen, L. Zou, K. B. Cordner, N. L. DelGaudio, V. Durani, M. Kini, M. Rex, H. S. Tian, J. Zuber, T. Baslan, S. W. Lowe, H. Y. Rienhoff, A. Letai, R. L. Levine, S. A. Armstrong, Leukemia cell of origin influences apoptotic priming and sensitivity to LSD1 inhibition. *Cancer Discov*, (2020); published online EpubJun 30 (10.1158/2159-8290.CD-19-1469).
64. S. Kane, Sample Size Calculator. ClinCalc: https://clincalc.com/Stats/SampleSize.aspx. (2019).
65. A. J. Deshpande, L. Chen, M. Fazio, A. U. Sinha, K. M. Bernt, D. Banka, S. Dias, J. Chang, E. J. Olhava, S. R. Daigle, V. M. Richon, R. M. Pollock, S. A. Armstrong, Leukemic transformation by the MLL-AF6 fusion oncogene requires the H3K79 methyltransferase Dot1l. *Blood* **121**, 2533-2541 (2013); published online EpubMar 28 (10.1182/blood-2012-11-465120).

66. M. T. Esposito, L. Zhao, T. K. Fung, J. K. Rane, A. Wilson, N. Martin, J. Gil, A. Y. Leung, A. Ashworth, C. W. So, Synthetic lethal targeting of oncogenic transcription factors in acute leukemia by PARP inhibitors. *Nat Med* **21**, 1481-1490 (2015); published online EpubDec (10.1038/nm.3993).
67. N. Cheung, T. K. Fung, B. B. Zeisig, K. Holmes, J. K. Rane, K. A. Mowen, M. G. Finn, B. Lenhard, L. C. Chan, C. W. So, Targeting Aberrant Epigenetic Networks Mediated by PRMT1 and KDM4C in Acute Myeloid Leukemia. *Cancer Cell* **29**, 32-48 (2016); published online EpubJan 11 (10.1016/j.ccell.2015.12.007).
68. J. Taminau *et al*., Unlocking the potential of publicly available microarray data using inSilicoDb and inSilicoMerging R/Bioconductor packages. *BMC Bioinformatics* **13**, 335 (2012).

Acknowledgements

We would like to dedicate this paper to the memory of Ms Amanda Wilson, the lab manager of So lab, for her important contributions to the execution of this work. We thank Farzin Farzaneh, Peter Parker, Chris Marine, and Florian Rambow for constructive comments on the manuscript; James Mulloy for advice on the transformation assay; Louis Chesler for in vivo luciferase reporter construct; Sam Tung, Kornelia Gladysz, and Haoli Li for bioinformatics input; Amanda Wilson, Anthony Eiliazadeh, Winston Vetharoy, and Alan Dunlop for assistance with mouse work and flow cytometry; Barbara Czepulkowski for FISH; Cancer Research UK (CRUK) King's Health Partners Centre and BRC at KCL for infrastructural and NGS support, respectively; Anthony Nolan for supply of human cord blood samples; Heidi Altmann and the Study Alliance Leukemia (www.sal-aml.org) for biobanking and sample provision; Donal Mclornan, Austin Kulasekararaj, Victoria Potter, and Nelson Ng for assistance with patient sample collections; and members of So lab for helpful discussion. Editorial services were provided by Nancy R. Gough (BioSerendipity, LLC) on behalf of AAAS.

Funding

CWES is a holder of an CRUK programme grant, a Blood Cancer UK research grant, a Kay Kendall Leukaemia Fund research grant, and a Royal Society Wolfson Research Merit Award. SH is supported by an NIH grant R01CA 204044.

Author Contributions

BBZ, TKF, CTT, BS performed experiments; MZ, CL, BBZ, BL, HL carried out bioinformatics analyses; AYHL, JZ, MZ, MB, MVB, GJM provided clinical samples and data; MZ, BL, AYHL, JZ, MZ, MB, MVB, GJM advised on manuscript preparation; BBZ, TKF, SH, CWES wrote and edited the manuscript; CWES conceptualized and oversaw the project.

Competing interests

All authors declare that they have no competing interests.

Data availability

All data associated with this study are present in the paper or the Supplementary Materials. RNA-seq data is deposited under E-MTAB-5501 (ArrayExpress). WGS data is deposited under Bioproject accession PRJNA601070.

Figure legends

Fig. 1. Human HSCs and CMPs but not LMPPs or GMPs are cellular targets for MLL fusion-mediated transformation. (**A**) Proliferation of cells in culture was measured as fold expansion each week for the normal and MLL-transformed populations of cells. ME, MLL-ENL; MA6, MLL-AF6. (**B**) Typical cell morphology at 4 – 6 weeks of in vitro culture of the indicated cell types. Scale bar = 10 µm. (**C**) NBT staining defining the percentage of myeloid-differentiated cells of indicated groups (n = 4/cell of origin). MLLx: MLL-ENL and MLL-AF6. P=1.25E-19, HSC-/CMP-MLLx vs LMPP-/GMP-MLLx. (**D**) Bar chart represents the percentage of cells in each category after AnnexinV and propidium staining of the indicated cells. Data are presented as mean ± SD, and statistical significance of p = 0.00319 was determined by ANOVA from N = 3, n = 6, F-value = 14.86, df = 1, for HSC-/CMP-MLLx vs LMPP-/GMP-MLLx. (**E**) Long-term culture initiating cell (LTC-IC) frequencies of the indicated groups at 4 weeks of in vitro culture (n = 6). (**F**) Typical surface marker abundance of the indicated transformed cell populations at 8 – 10 weeks in culture. (**G**) Venn diagram showing the overlap of significantly differentially expressed genes between HSC/CMP-MLLx and LMPP/GMP-MLLx cells using DEseq2, ANOVA (on rlog transformed read counts) and ANOVA (on vst transformed read counts) as indicated. (**H**) Heatmap showing the 130 genes with consistently higher expression in LMPP/GMP-MLLx, and the 45 genes with consistently higher expression in HSC/CMP-MLLx and their functional annotations according to webgestalt and Toppgene. (**I**) Selected stem cell-related gene sets from GSEA are shown comparing HSC-/CMP-MLLx (HC-MLLx) and LMPP-/GMP-MLLx (LG/MLLx) cells. In panels A, C, and E, data are represented as mean ± SD. In panels C and E, statistical significance was determined by student t-test.

Fig. 2. HSC-MLLx and CMP-MLLx cells induce AML with CSCs residing in the CD34$^{-/lo}$CD38^{+} population. (**A)** Kaplan-Meier survival curves for NSG mice injected with the

indicated MLLx-transformed populations. Log-rank test showed $p < 0.0001$ HSC-ME versus CMP-ME and $p = 0.47$ HSC-MA6 versus CMP-MA6. ME, MLL-ENL; MA6, MLL-AF6. (**B**) Comparison of blood, spleen, and liver from primary leukemic mice injected with the indicated cell type. Top: May-Gruenwald/Giemsa stained peripheral blood smear, scale bar = 10 µm. Middle: H&E stained spleen section, scale bar = 100 µm. Bottom: H&E stained liver section, scale bar = 100 µm. Dark purple stained cells indicate leukemic blasts. **(C)** Long-term culture-initiating cell (LTC-IC) frequencies of the indicated CD34/CD38 populations sorted from transformed MLL-ENL and MLL-AF6 (MLLx) cell lines are shown. Pooled results for both HSC-transformed cells and for both CMP-transformed cells are shown mean ± SD. LTC-IC frequency of each fraction was normalized to that of the unsorted cells (bulk). Statistical significance was determined by student t-test (n = 5 per CD34/CD38 population). (**D**) In vivo limiting dilution assay of indicated sorted CD34/CD38 populations isolated from primary leukemic mice injected with CD34-CD38+ or CD34+CD38+ cells. Solid lines are their calculated frequency; dotted lines are the upper and lower range of frequencies within confidence intervals.

Fig. 3. CSCs are highly enriched in the $CD34^{-/lo}CD38^{+}$ compartment in patients with MLL-AML. (**A), (B**) LTC-IC frequencies of sorted CD34/CD38 populations in MLL-AML patient samples from the (A) $CD34^{-/lo}$ group (n=3) or (B) $CD34^{+}$ group (n=6). Data are presented normalized to the unsorted cell populations (bulk). Data mean ± SD and statistical significance was determined by student t-test. (**C), (D**) Kaplan-Meyer survival curves for NSG mice transplanted with the indicated sorted CD34/CD38 populations from (C) patient M519 in the $CD34^{-/lo}$ group: $CD34^{-}CD38^{+}$, 5 mice; $CD34^{+}CD38^{+}$, 3 mice; $CD34^{-}CD38^{-}$, 4 mice or (D) patient HMW in the $CD34^{+}$ group: $CD34^{-}CD38^{+}$, 4 mice; $CD34^{+}CD38^{-}$, 5 mice; $CD34^{+}CD38^{+}$, 4 mice; $CD34^{-}CD38^{-}$, 3 mice. Log-rank test showed $p < 0.05$ for $CD34^{-}CD38^{+}$ versus any other fraction in both C and D. (**E), (F**) In vivo limiting dilution assay of indicated CD34/CD38

population sorted from samples from patients with MLL-AML in the (E) $CD34^{-/lo}$ group or (F) $CD34^{+}$ group. Patient identifier is above the graphs. Upper graphs: the log fraction non responding is shown; lower graphs: the LSC enrichment over bulk is shown. (**G), (H**) Percentage of $CD34^{+}$ cells (upper graphs) and $CD34^{-}CD38^{+}$ cells (lower graphs) in patient samples and the corresponding matched populations after engraftment in mice. (G) Unsorted (bulk) cells were used from patients with MLL-AML in the $CD34^{-/lo}$ group (n = 4 patients; left) and $CD34^{+}$ group (n = 6 patients; right). (H) Sorted $CD34^{-}CD38^{+}$ cells were used from patients with MLL-AML in the $CD34^{-/lo}$ group (n = 4 patients; left) and $CD34^{+}$ group (n = 4 patients; right). Each line represents one mouse and the black bars represent the mean. Statistical significance was determined by student t-test.

Fig. 4. Human HSCs-derived MLL-AML is more resistant to chemotherapy than is CMP-derived MLL-AML. (**A**) Kaplan-Meier survival curves are shown for patients with AML classified as HSC-like (red) and CMP-like (blue) using a machine learning approach. Median survival and log-rank-test p-value are indicated. (**B)** LTC-IC frequency of HSC-MLLx (n = 4) or CMP-MLLx (n=4) cell lines. Cells were exposed to cytarabine (Ara-C) or DOXO for 1 week and data are presented relative to untreated control cells. (**C**) Bar chart represents the response of mice treated with DOXO as measured by bio-imaging. Mice were transplanted with HSC-MLL-ENL (HSC-ME) or CMP-MLL-ENL (CMP-ME) cells and either treated with or without DOXO. Data are presented relative to the control mice (n=5 mice/group). **(D)** LTC-IC frequency of HSC-like (n=7; 6 individual samples) or CMP-like (n=3; 2 individual samples) cells from patients with MLL-AML. Cells were exposed to cytarabine or DOXO for 1 week and data are presented relative to untreated control cells. (**E**) Kaplan-Meier survival curves are shown for mice transplanted with cells from patients with HSC-like or CMP-like MLL-AML and then treated with DOXO (chemo) or without (control). Log-rank test showed $p < 0.05$ CMP-like chemo versus CMP-like control (n = 4 mice in control groups and 5 mice in DOXO-

treated groups). In panels B, C, and D, data are represented as mean ± SD and statistical significance was determined by student t-test.

Fig. 5. ABCC3 is a candidate target for chemoresistant HSC-derived MLL-AML. (**A**) Heatmap of the 99 genes differentially expressed between HSC-MLLx and CMP-MLLx with genes *ABCC3* and *IL6* highlighted as the genes also found with GEAR database. (**B**) LTC-IC frequency of HSC-MLLx cell lines upon the DOXO treatment with or without ABCC3 knockdown (sh ABCC3) is shown (n = 6). LKO, vector control. (**C**) Pulse-chase experiment with HSC-derived MLL cell line and Fluo-8AM. (Left) Flow cytometry plot with red curve indicating cells incubated for 30 min with Fluo8-AM (pulse) and black as the control cells without Fluo-8AM. (Middle) Flow cytometry plots for cells chased for the indicated times in the presence of DMSO (control, top row) or in fidaxomicin (FIDA, 5 μM). Red curves indicate the maximum intensity of fluorescence at the end of the 30 min pulse; blue curves indicate the fluorescence intensity at the indicated timepoint. (Right) Bar chart represents the mean fluorescence intensity at the indicated time points with or without fidaxomicin treatment (n = 4). **(D)** Bar chart represents the mean fluorescence intensity at the indicated time points for HSC-MLLx cell lines with or without ABCC3 knockdown (n = 9). ABCC knockdown, sh403 and sh406; LKO, vector control. (**E**) LTC-IC frequency of HSC-MLLx cell lines upon the indicated treatments relative to the mock-control is shown (n = 5). (**F**) In vivo luciferase imaging of NSG mice transplanted with HSC-MLL-MA6. Mice were treated with fidaxomicin, DOXO or a combination of both. Imaging was performed pre-treatment (day 14 after transplant) and post-treatment (day 1 after last treatment). All 5 mice in each group are shown. Bar chart indicates the ratio of the measured radiance post-/pre-treatment. The red dashed line represents a post/pre ratio of 1. In panels B, C, D, E, and F, data are represented as mean ± SD and statistical significance was determined by student t-test.

Fig. 6. Fidaxomicin overcomes chemoresistance associated with stem cell origins in primary AML patient samples. (**A-D**) Primary MLL-AML patient samples of predicted HSC origin were treated with the indicated drugs and subjected to various in vitro assays. The bar charts present (A) the number of viable cells by cell counting (n = 4; 4 individual patient samples); (B) LTC-IC assay showing LTC-IC frequencies (n = 4; 4 individual patient samples); (C) NBT reduction assay showing the relative numbers of NBT^+ cells (n = 4; 4 individual patient samples); and (D) apoptosis assay showing the percentage of Annexin V^+ (AnV+) cells (n = 3; 3 individual patient samples). Data are represented as mean ± SD. Statistical significance was determined by student t-test. (**E**) In vivo luciferase imaging of NSG mice transplanted with primary MLL-AML cells of predicted HSC origin from patient sample #1. Mice were treated with DOXO, fidaxomicin, or a combination of both. Imaging was performed pre-treatment (day 20 after transplant) and post-treatment (day 1 after last treatment). All 5 mice in each group are shown. (**F**) Kaplan-Meier survival curves are shown for indicated mice treated with DOXO, fidaxomicin, combination or control. Mice were transplanted with HSC-like cells from MLL-AML patient #1. Log-rank test showed p=0.2 comparing DOXO treatment against control and $p < 0.01$ comparing the DOXO and fidaxomicin combination treatment against any other treatment (n = 5 mice/group). (**G**) Bone marrow aspiration of NSG mice transplanted with HSC-like MLL-AML cells from patient #2. Mice were treated with fidaxomicin, DOXO, or the combination (n = 5 mice/group). Significance was determined by student t-test. **(H**) Kaplan-Meier survival curves are shown for mice receiving the indicated DOXO, fidaxomicin, combination or control treatment. Mice were transplanted with HSC-like MLL-AML cells from patient #2. Log-rank test showed $p < 0.01$ comparing DOXO and fidaxomicin combination treatment against any other treatment (n = 5 mice/group).

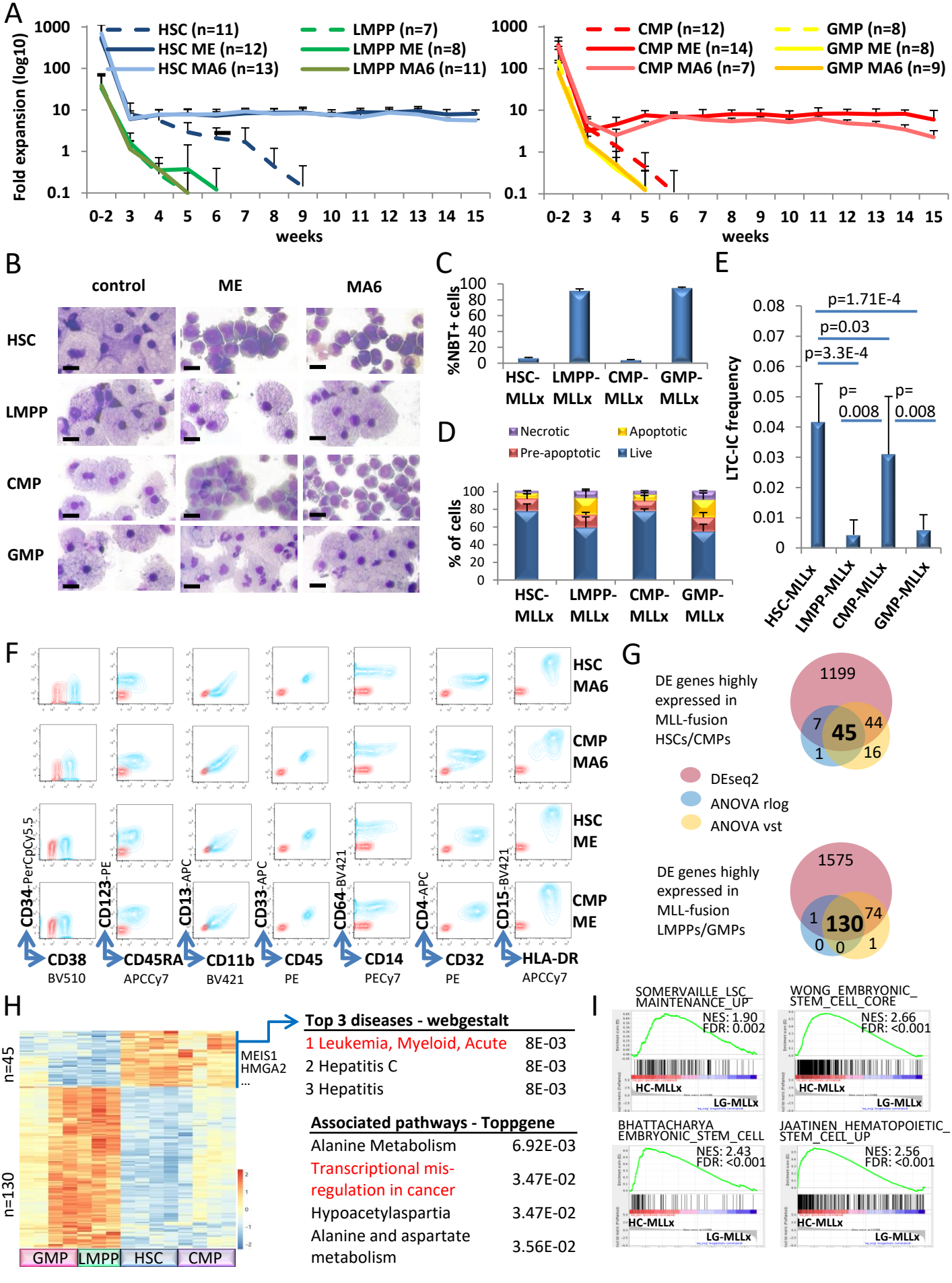
A
Fold expansion (log10)
1000
100
10
1
0.1
HSC (n=11)
HSC ME (n=12)
HSC MA6 (n=13)
LMPP (n=7)
LMPP ME (n=8)
LMPP MA6 (n=11)
0-2 3 4 5 6 7 8 9 10 11 12 13 14 15
weeks
CMP (n=12)
CMP ME (n=14)
CMP MA6 (n=7)
GMP (n=8)
GMP ME (n=8)
GMP MA6 (n=9)
B
control
ME
MA6
HSC
LMPP
CMP
GMP
C
%NBT+ cells
100
80
60
40
20
0
HSC-MLLx
LMPP-MLLx
CMP-MLLx
GMP-MLLx
D
Necrotic
Apoptotic
Pre-apoptotic
Live
% of cells
E
LTC-IC frequency
0.08
0.07
0.06
0.05
0.04
0.03
0.02
0.01
0
p=1.71E-4
p=0.03
p=3.3E-4
p= 0.008
p= 0.008
HSC-MLLx
LMPP-MLLx
CMP-MLLx
GMP-MLLx
F
HSC MA6
CMP MA6
HSC ME
CMP ME
CD34-PerCpCy5.5
CD123-PE
CD13-APC
CD33-APC
CD64-BV421
CD4-APC
CD15-BV421
CD38 BV510
CD45RA APCCy7
CD11b BV421
CD45 PE
CD14 PECy7
CD32 PE
HLA-DR APCCy7
G
DE genes highly expressed in MLL-fusion HSCs/CMPs
1199
7
45
44
1
16
DEseq2
ANOVA rlog
ANOVA vst
DE genes highly expressed in MLL-fusion LMPPs/GMPs
1575
1
130
74
0
0
1
H
n=45
n=130
MEIS1
HMGA2
...
GMP
LMPP
HSC
CMP
Top 3 diseases - webgestalt
1 Leukemia, Myeloid, Acute 8E-03
2 Hepatitis C 8E-03
3 Hepatitis 8E-03
Associated pathways - Toppgene
Alanine Metabolism 6.92E-03
Transcriptional mis-regulation in cancer 3.47E-02
Hypoacetylaspartia 3.47E-02
Alanine and aspartate metabolism 3.56E-02
I
SOMERVAILLE_LSC MAINTENANCE_UP
NES: 1.90
FDR: 0.002
HC-MLLx
LG-MLLx
WONG_EMBRYONIC_ STEM_CELL_CORE
NES: 2.66
FDR: <0.001
BHATTACHARYA EMBRYONIC_STEM_CELL
NES: 2.43
FDR: <0.001
JAATINEN_HEMATOPOIETIC_ STEM_CELL_UP
NES: 2.56
FDR: <0.001

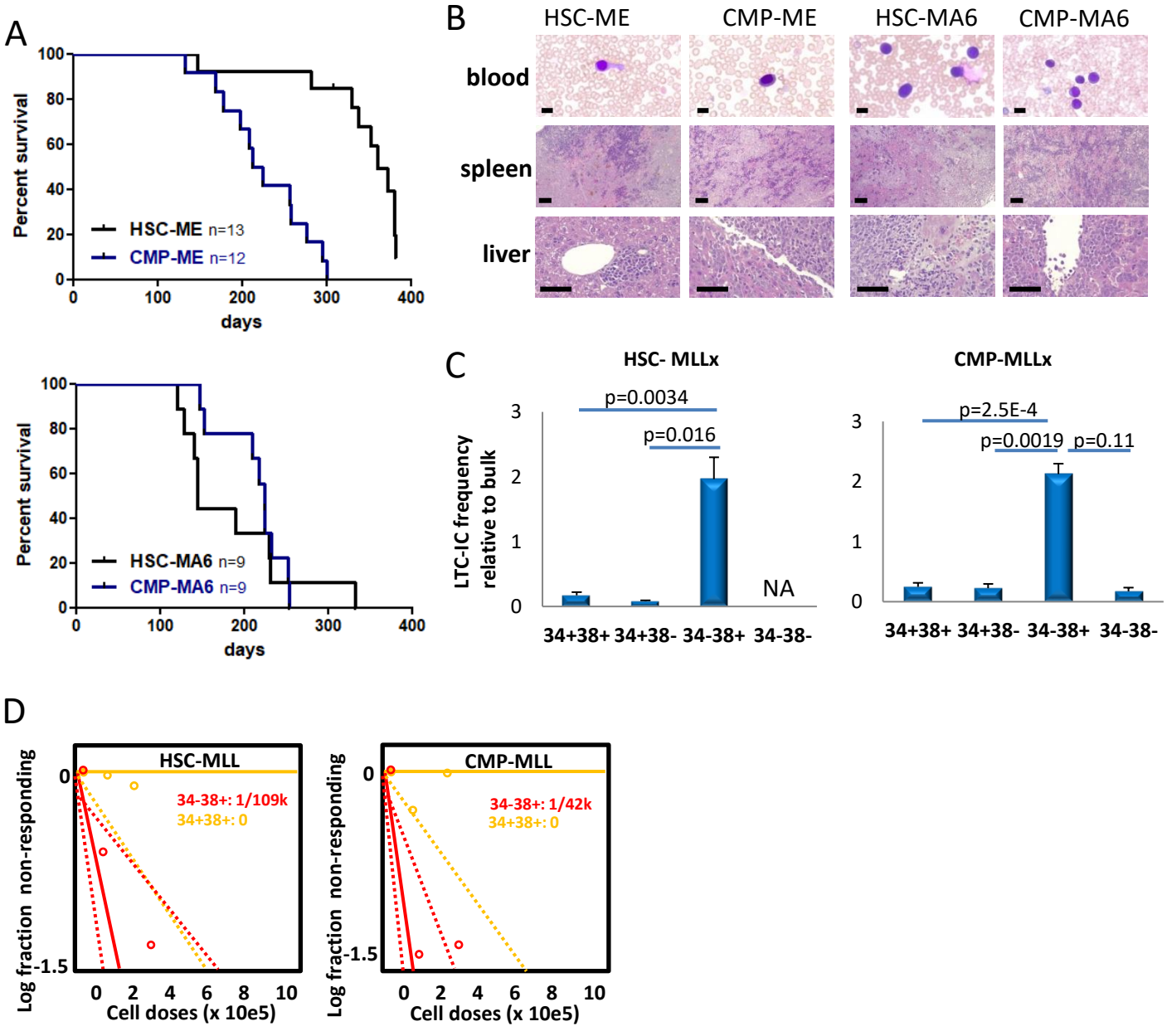
A
Percent survival
HSC-ME n=13
CMP-ME n=12
days
HSC-MA6 n=9
CMP-MA6 n=9
B
HSC-ME
CMP-ME
HSC-MA6
CMP-MA6
blood
spleen
liver
C
HSC- MLLx
CMP-MLLx
LTC-IC frequency relative to bulk
p=0.0034
p=0.016
NA
p=2.5E-4
p=0.0019
p=0.11
34+38+
34+38-
34-38+
34-38-
D
HSC-MLL
34-38+: 1/109k
34+38+: 0
CMP-MLL
34-38+: 1/42k
34+38+: 0
Log fraction non-responding
Cell doses (x 10e5)

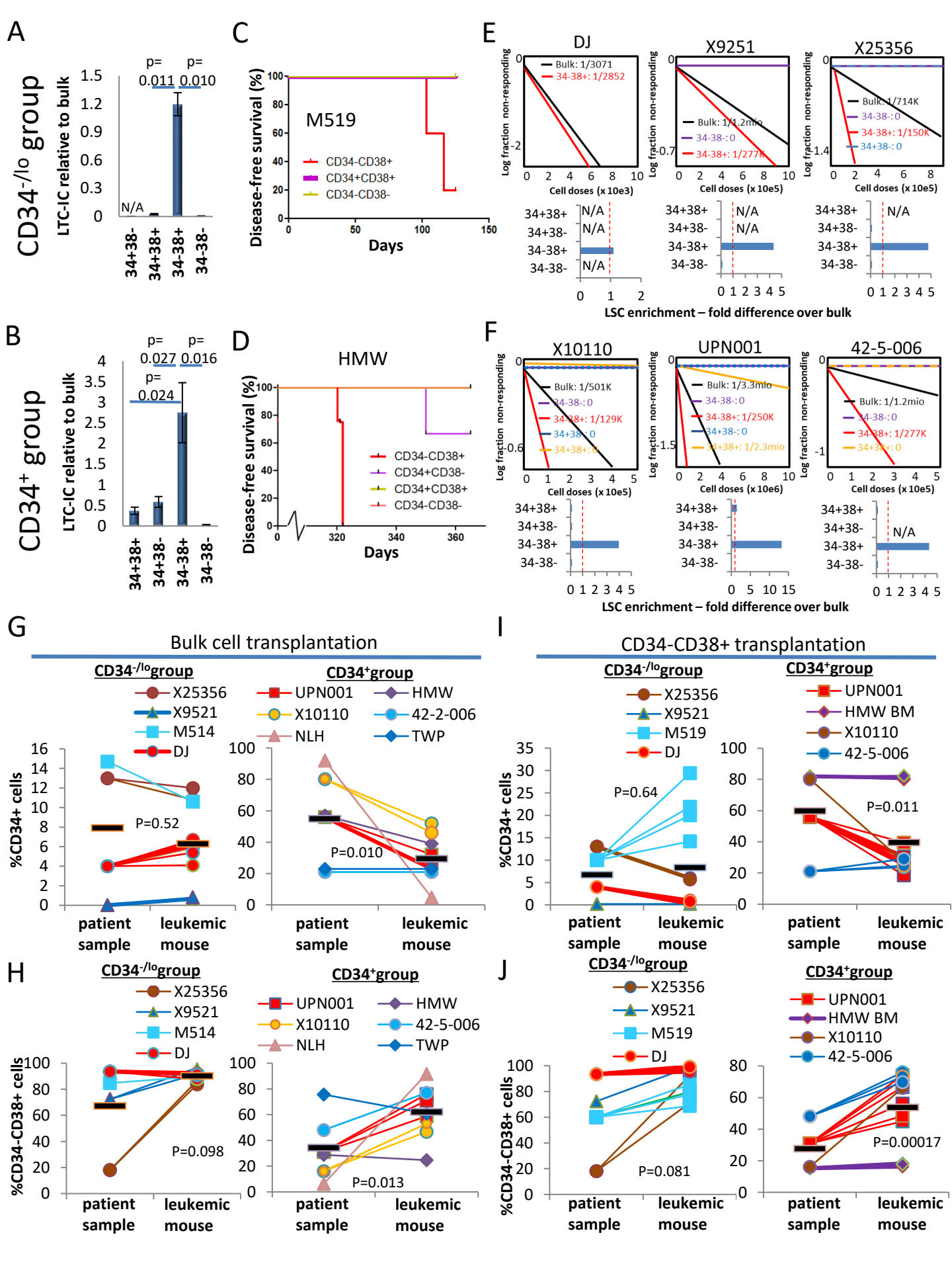
A
CD34-/lo group
LTC-IC relative to bulk
p= 0.011
p= 0.010
N/A
34+38+
34+38+
34-38+
34-38-
C
Disease-free survival (%)
M519
CD34-CD38+
CD34+CD38+
CD34-CD38-
Days
E
DJ
X9251
X25356
Log fraction non-responding
Bulk: 1/3071
34-38+: 1/2852
Bulk: 1/1.2mio
34-38-: 0
34-38+: 1/277K
Bulk: 1/714K
34-38-: 0
34-38+: 1/150K
34+38-: 0
Cell doses (x 10e3)
Cell doses (x 10e5)
34+38+
34+38-
34-38+
34-38-
N/A
LSC enrichment – fold difference over bulk
B
CD34+ group
LTC-IC relative to bulk
p= 0.027
p= 0.016
p= 0.024
34+38+
34+38-
34-38+
34-38-
D
HMW
Disease-free survival (%)
CD34-CD38+
CD34+CD38-
CD34+CD38+
CD34-CD38-
Days
F
X10110
UPN001
42-5-006
Bulk: 1/501K
34-38-: 0
34-38+: 1/129K
34+38-: 0
34+38+: 0
Bulk: 1/3.3mio
34-38-: 0
34-38+: 1/250K
34+38-: 0
34+38+: 1/2.3mio
Bulk: 1/1.2mio
34-38-: 0
34-38+: 1/277K
34+38+: 0
Cell doses (x 10e6)
LSC enrichment – fold difference over bulk
G
Bulk cell transplantation
CD34-/lo group
CD34+ group
X25356
X9521
M514
DJ
UPN001
X10110
NLH
HMW
42-2-006
TWP
%CD34+ cells
P=0.52
P=0.010
patient sample
leukemic mouse
I
CD34-CD38+ transplantation
M519
HMW BM
P=0.64
P=0.011
H
%CD34-CD38+ cells
P=0.098
P=0.013
J
P=0.081
P=0.00017

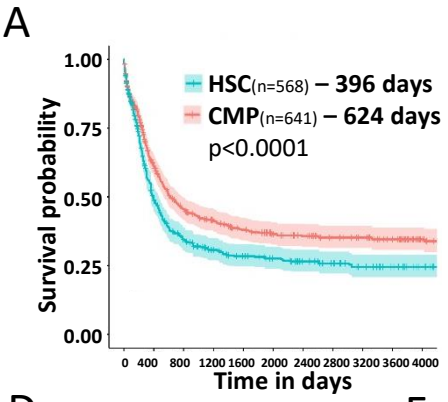
A
Survival probability
1.00
0.75
0.50
0.25
0.00
HSC(n=568) – 396 days
CMP(n=641) – 624 days
p<0.0001
0 400 800 1200 1600 2000 2400 2800 3200 3600 4000
Time in days

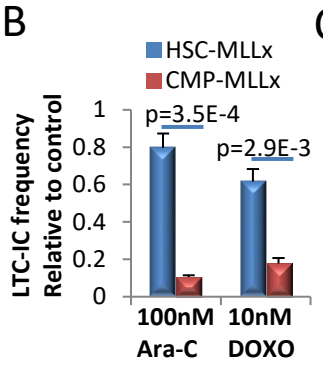
B
HSC-MLLx
CMP-MLLx
LTC-IC frequency
Relative to control
1
0.8
0.6
0.4
0.2
0
p=3.5E-4
p=2.9E-3
100nM
Ara-C
10nM
DOXO

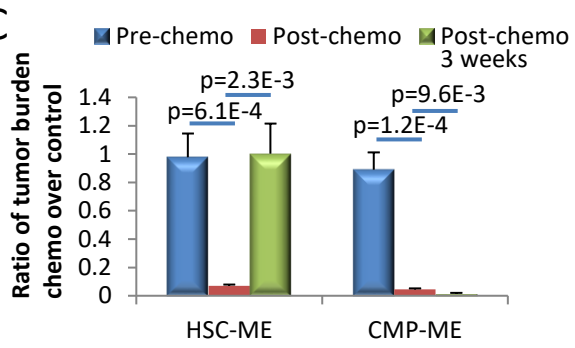
C
Pre-chemo
Post-chemo
Post-chemo
3 weeks
Ratio of tumor burden
chemo over control
1.4
1.2
1
0.8
0.6
0.4
0.2
0
p=2.3E-3
p=6.1E-4
p=9.6E-3
p=1.2E-4
HSC-ME
CMP-ME

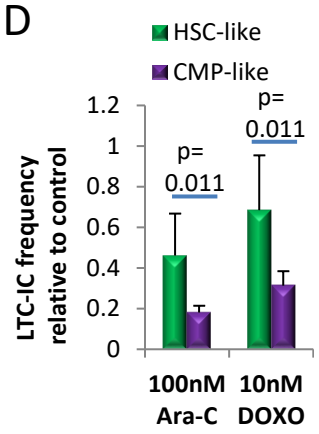
D
HSC-like
CMP-like
LTC-IC frequency
relative to control
1.2
1
0.8
0.6
0.4
0.2
0
p=
0.011
p=
0.011
100nM
Ara-C
10nM
DOXO

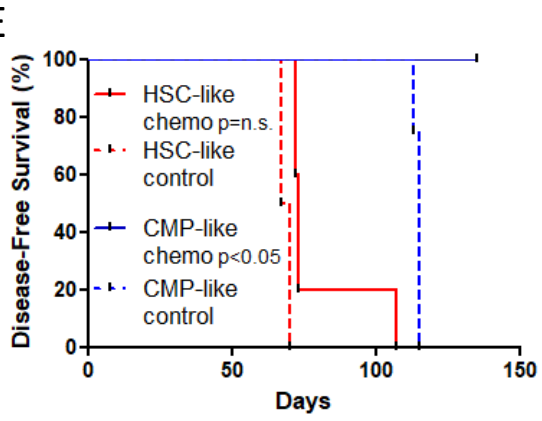
E
Disease-Free Survival (%)
100
80
60
40
20
0
HSC-like
chemo p=n.s.
HSC-like
control
CMP-like
chemo p<0.05
CMP-like
control
0
50
100
150
Days

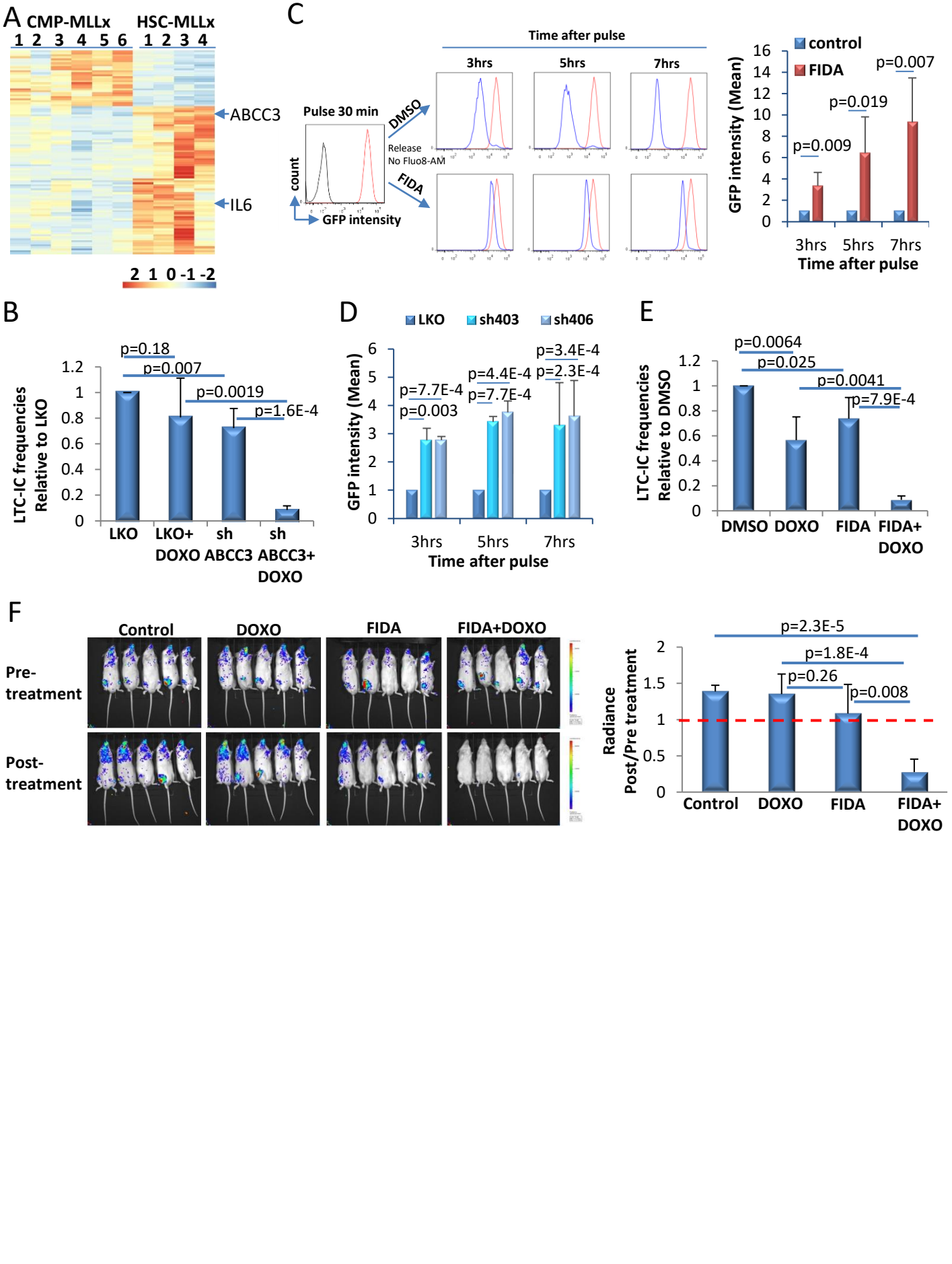
A
CMP-MLLx
HSC-MLLx
1 2 3 4 5 6
1 2 3 4
ABCC3
IL6
2 1 0 -1 -2
C
Time after pulse
3hrs
5hrs
7hrs
Pulse 30 min
DMSO
Release
No Fluo8-AM
FIDA
count
GFP intensity
control
FIDA
GFP intensity (Mean)
p=0.009
p=0.019
p=0.007
3hrs
5hrs
7hrs
Time after pulse
B
LTC-IC frequencies
Relative to LKO
p=0.18
p=0.007
p=0.0019
p=1.6E-4
LKO
LKO+
DOXO
sh
ABCC3
sh
ABCC3+
DOXO
D
LKO
sh403
sh406
GFP intensity (Mean)
p=7.7E-4
p=0.003
p=4.4E-4
p=7.7E-4
p=3.4E-4
p=2.3E-4
3hrs
5hrs
7hrs
Time after pulse
E
LTC-IC frequencies
Relative to DMSO
p=0.0064
p=0.025
p=0.0041
p=7.9E-4
DMSO
DOXO
FIDA
FIDA+
DOXO
F
Control
DOXO
FIDA
FIDA+DOXO
Pre-
treatment
Post-
treatment
Radiance
Post/Pre treatment
p=2.3E-5
p=1.8E-4
p=0.26
p=0.008
Control
DOXO
FIDA
FIDA+
DOXO

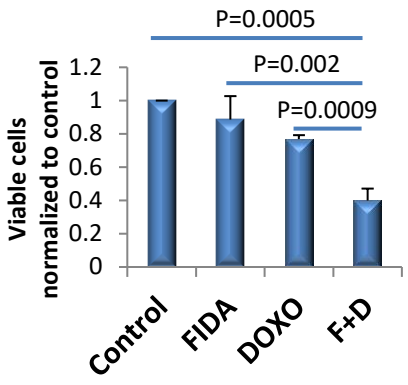
P=0.0005
P=0.002
P=0.0009
Viable cells normalized to control
1.2
1
0.8
0.6
0.4
0.2
0
Control
FIDA
DOXO
F+D

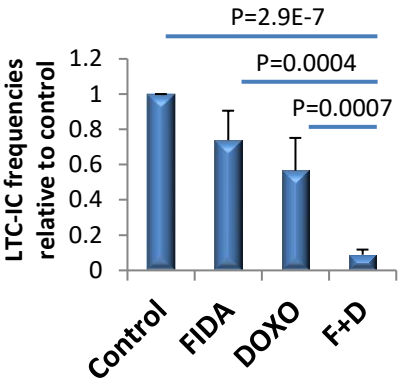
P=2.9E-7
P=0.0004
P=0.0007
LTC-IC frequencies relative to control
1.2
1
0.8
0.6
0.4
0.2
0
Control
FIDA
DOXO
F+D

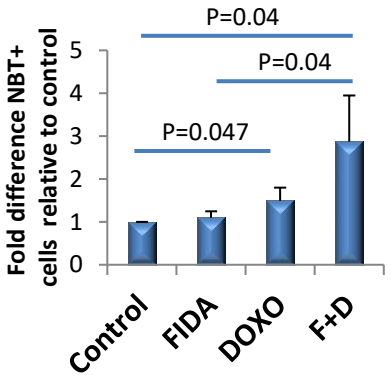
P=0.04
P=0.04
P=0.047
Fold difference NBT+ cells relative to control
5
4
3
2
1
0
Control
FIDA
DOXO
F+D

D

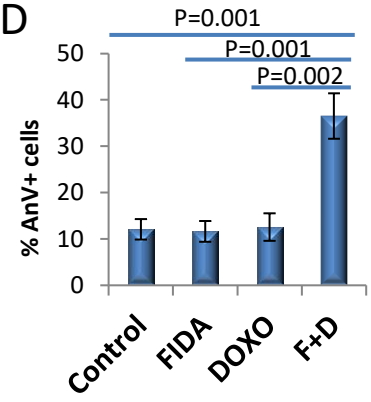
P=0.001
P=0.001
P=0.002
% AnV+ cells
50
40
30
20
10
0
Control
FIDA
DOXO
F+D

E

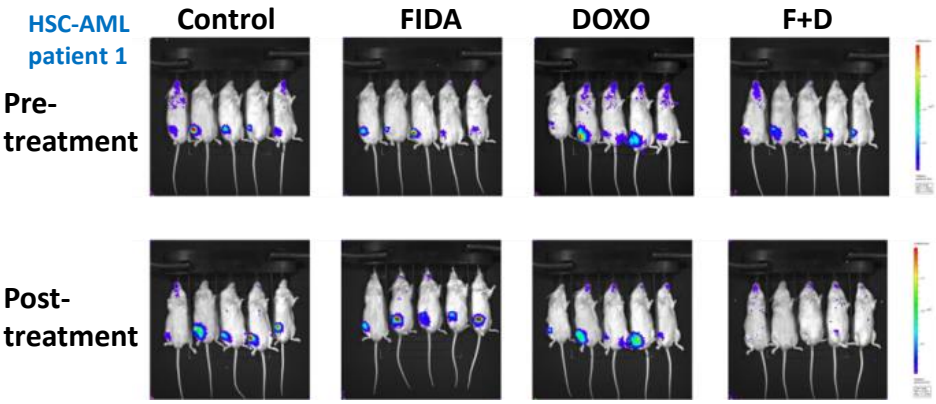
HSC-AML patient 1
Control
FIDA
DOXO
F+D
Pre-treatment
Post-treatment

F

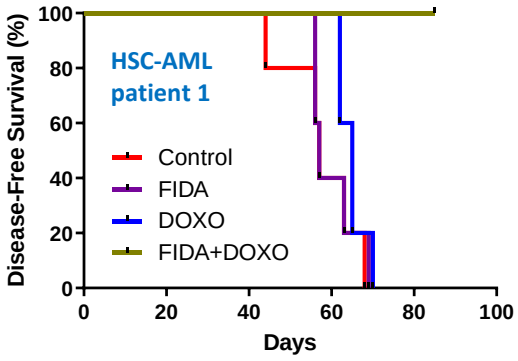
HSC-AML patient 1
Control
FIDA
DOXO
FIDA+DOXO
Disease-Free Survival (%)
100
80
60
40
20
0
0
20
40
60
80
100
Days

G

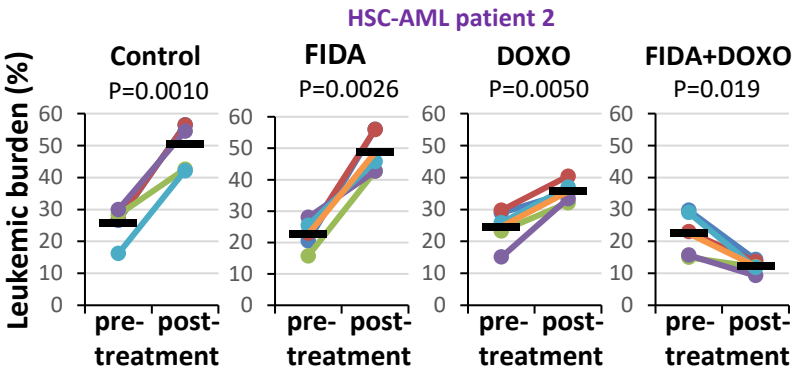
HSC-AML patient 2
Control
P=0.0010
FIDA
P=0.0026
DOXO
P=0.0050
FIDA+DOXO
P=0.019
Leukemic burden (%)
60
50
40
30
20
10
0
pre-treatment
post-treatment

H

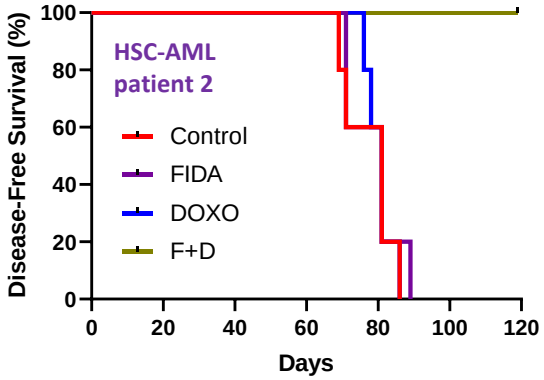
HSC-AML patient 2
Control
FIDA
DOXO
F+D
Disease-Free Survival (%)
100
80
60
40
20
0
0
20
40
60
80
100
120
Days

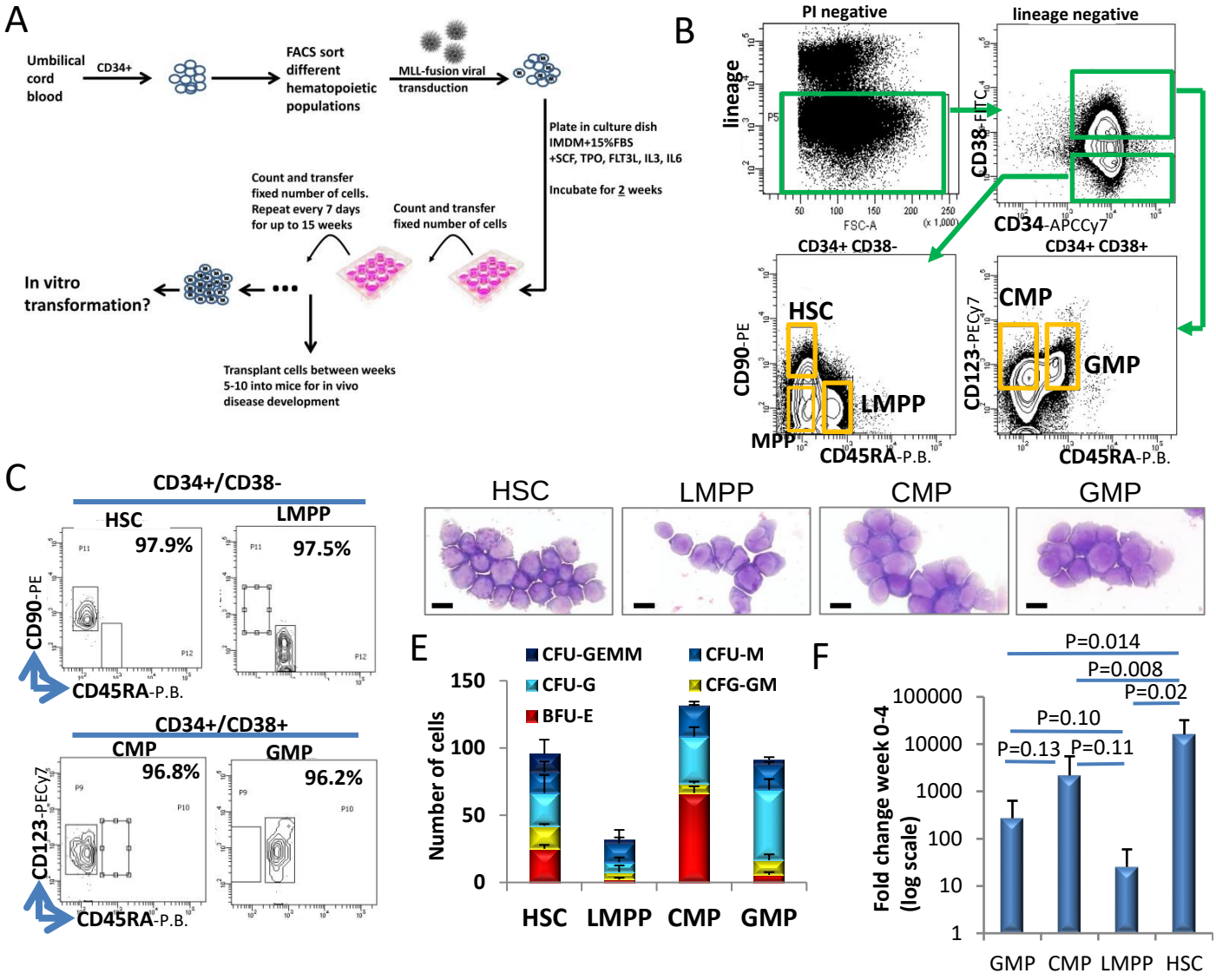
A
Umbilical cord blood
CD34+
FACS sort different hematopoietic populations
MLL-fusion viral transduction
Plate in culture dish IMDM+15%FBS +SCF, TPO, FLT3L, IL3, IL6
Incubate for 2 weeks
Count and transfer fixed number of cells. Repeat every 7 days for up to 15 weeks
Count and transfer fixed number of cells
In vitro transformation?
Transplant cells between weeks 5-10 into mice for in vivo disease development
B
PI negative
lineage negative
lineage
P5
FSC-A
CD38-FITC
CD34-APCCy7
CD34+ CD38-
CD34+ CD38+
HSC
LMPP
MPP
CMP
GMP
CD90-PE
CD123-PECy7
CD45RA-P.B.
C
CD34+/CD38-
HSC
LMPP
97.9%
97.5%
CD90-PE
CD45RA-P.B.
CD34+/CD38+
CMP
GMP
96.8%
96.2%
CD123-PECy7
CD45RA-P.B.
HSC
LMPP
CMP
GMP
E
CFU-GEMM
CFU-M
CFU-G
CFG-GM
BFU-E
Number of cells
150
100
50
0
HSC
LMPP
CMP
GMP
F
P=0.014
P=0.008
P=0.02
P=0.10
P=0.13
P=0.11
Fold change week 0-4 (log scale)
100000
10000
1000
100
10
1
GMP
CMP
LMPP
HSC

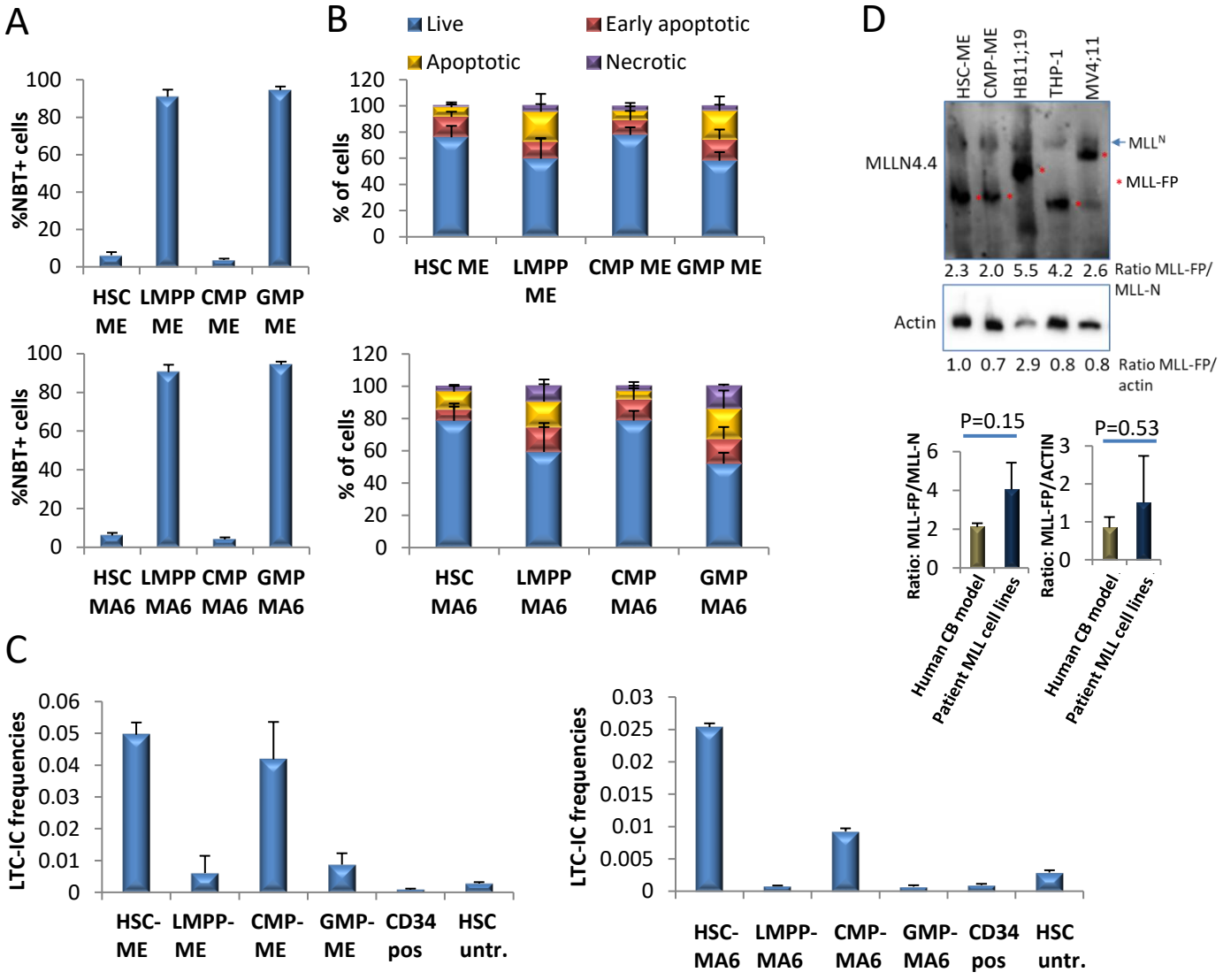
A
%NBT+ cells
HSC ME
LMPP ME
CMP ME
GMP ME
HSC MA6
LMPP MA6
CMP MA6
GMP MA6
B
Live
Early apoptotic
Apoptotic
Necrotic
% of cells
HSC ME
LMPP ME
CMP ME
GMP ME
HSC MA6
LMPP MA6
CMP MA6
GMP MA6
D
HSC-ME
CMP-ME
HB11;19
THP-1
MV4;11
MLLN4.4
MLL^N
MLL-FP
2.3 2.0 5.5 4.2 2.6 Ratio MLL-FP/ MLL-N
Actin
1.0 0.7 2.9 0.8 0.8 Ratio MLL-FP/ actin
P=0.15
Ratio: MLL-FP/MLL-N
Human CB model
Patient MLL cell lines
P=0.53
Ratio: MLL-FP/ACTIN
Human CB model
Patient MLL cell lines
C
LTC-IC frequencies
HSC-ME
LMPP-ME
CMP-ME
GMP-ME
CD34 pos
HSC untr.
LTC-IC frequencies
HSC-MA6
LMPP-MA6
CMP-MA6
GMP-MA6
CD34 pos
HSC untr.

A

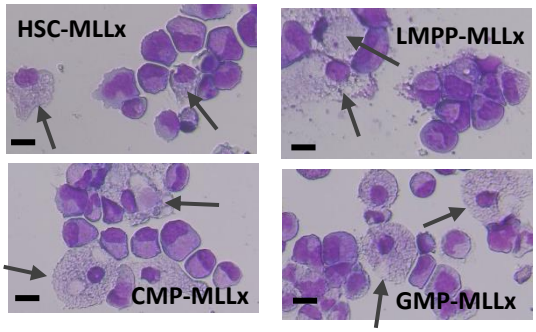

B

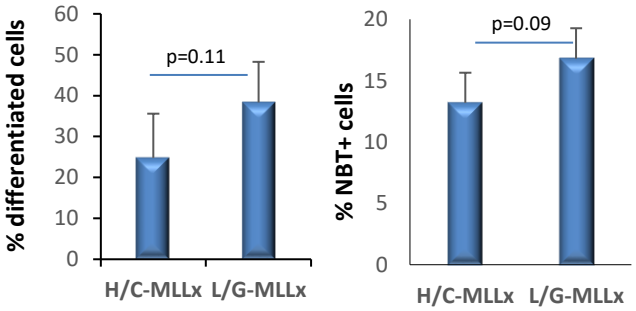

C

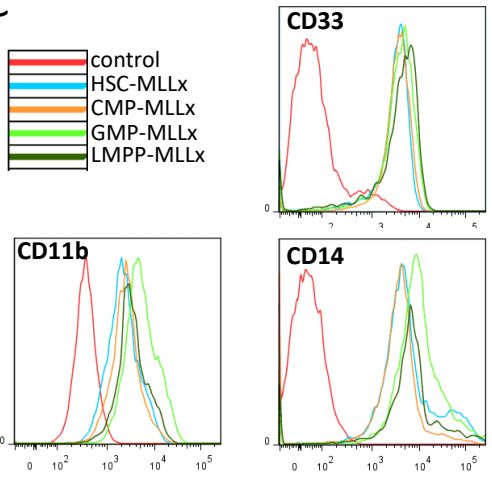

D

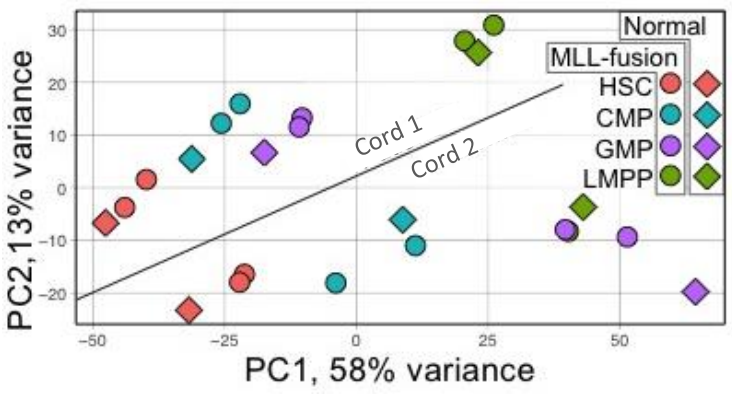

E

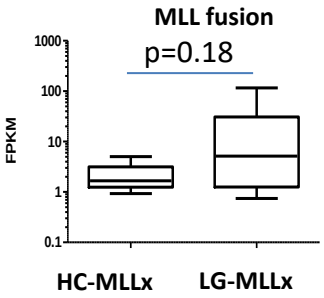

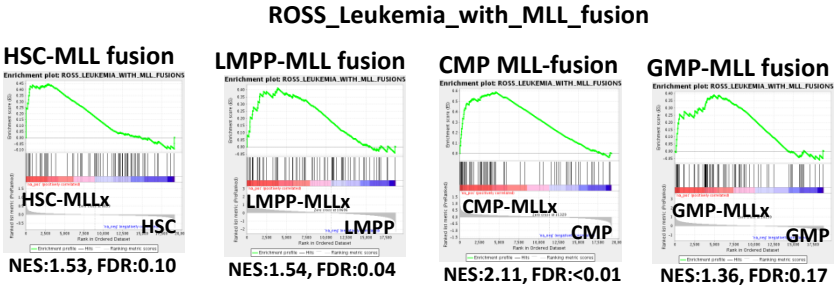

F

G

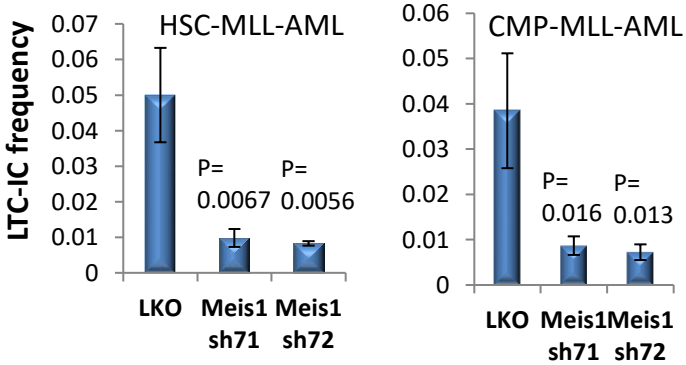

H

130 gene signature

Top 3 diseases - webgestalt

1 Nervous System Diseases
2 Inflammation
3 Lung Diseases, Obstructive

Associated Gene Family – Toppgene

Name	FDR B&H
CD molecules	1.34E-02
Potassium channels	1.44E-02
Kinesins	2.51E-02

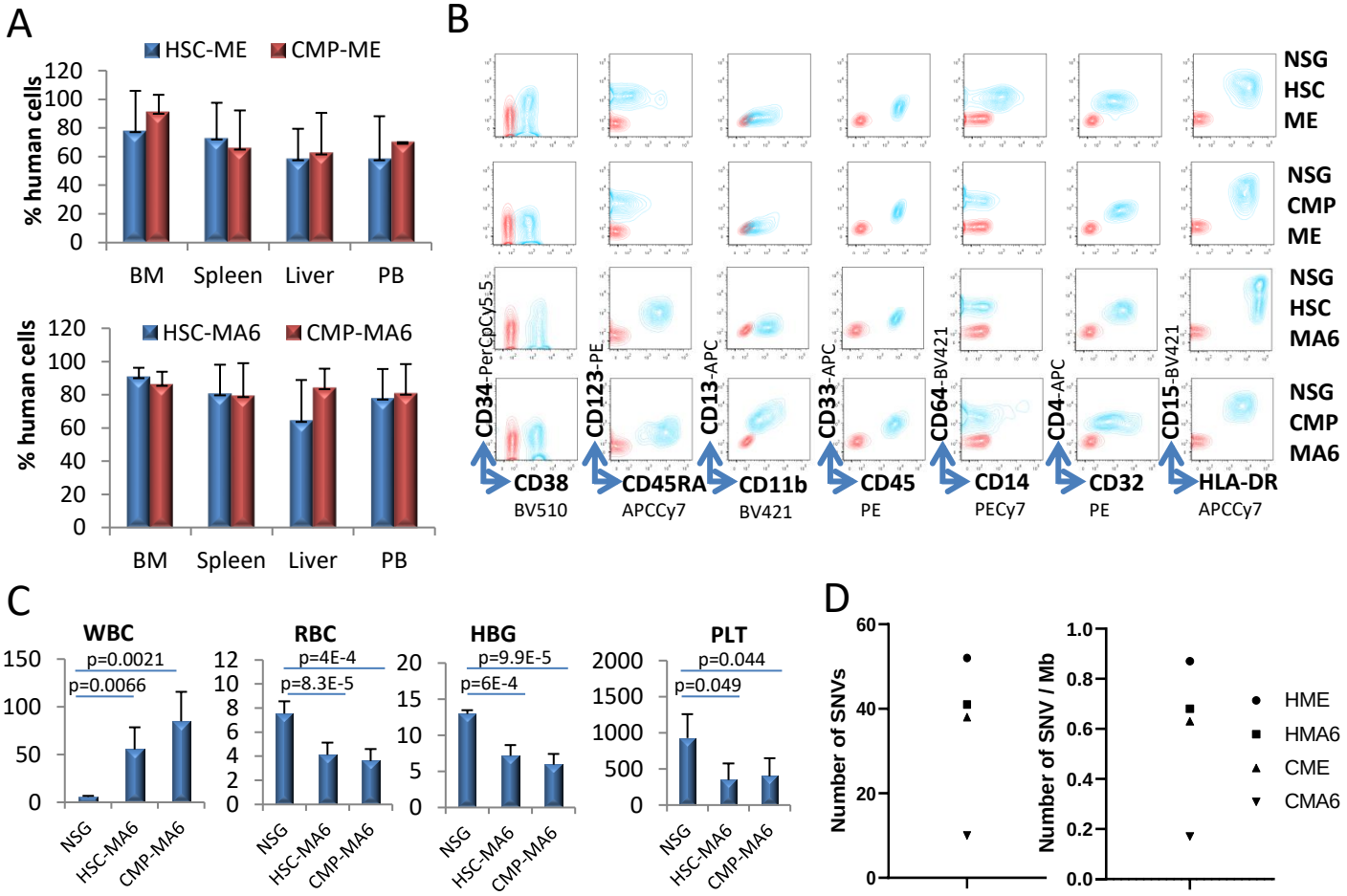
A
HSC-ME
CMP-ME
% human cells
120
100
80
60
40
20
0
BM
Spleen
Liver
PB
HSC-MA6
CMP-MA6
% human cells
120
100
80
60
40
20
0
BM
Spleen
Liver
PB
B
NSG HSC ME
NSG CMP ME
NSG HSC MA6
NSG CMP MA6
CD34-PerCpCy5-5
CD123-PE
CD13-APC
CD33-APC
CD64-BV421
CD4-APC
CD15-BV421
CD38 BV510
CD45RA APCCy7
CD11b BV421
CD45 PE
CD14 PECy7
CD32 PE
HLA-DR APCCy7
C
WBC
p=0.0021
p=0.0066
150
100
50
0
RBC
p=4E-4
p=8.3E-5
12
10
8
6
4
2
0
HBG
p=9.9E-5
p=6E-4
20
15
10
5
0
PLT
p=0.044
p=0.049
2000
1500
1000
500
0
NSG
HSC-MA6
CMP-MA6
D
Number of SNVs
60
40
20
0
Number of SNV / Mb
1.0
0.8
0.6
0.4
0.2
0.0
HME
HMA6
CME
CMA6

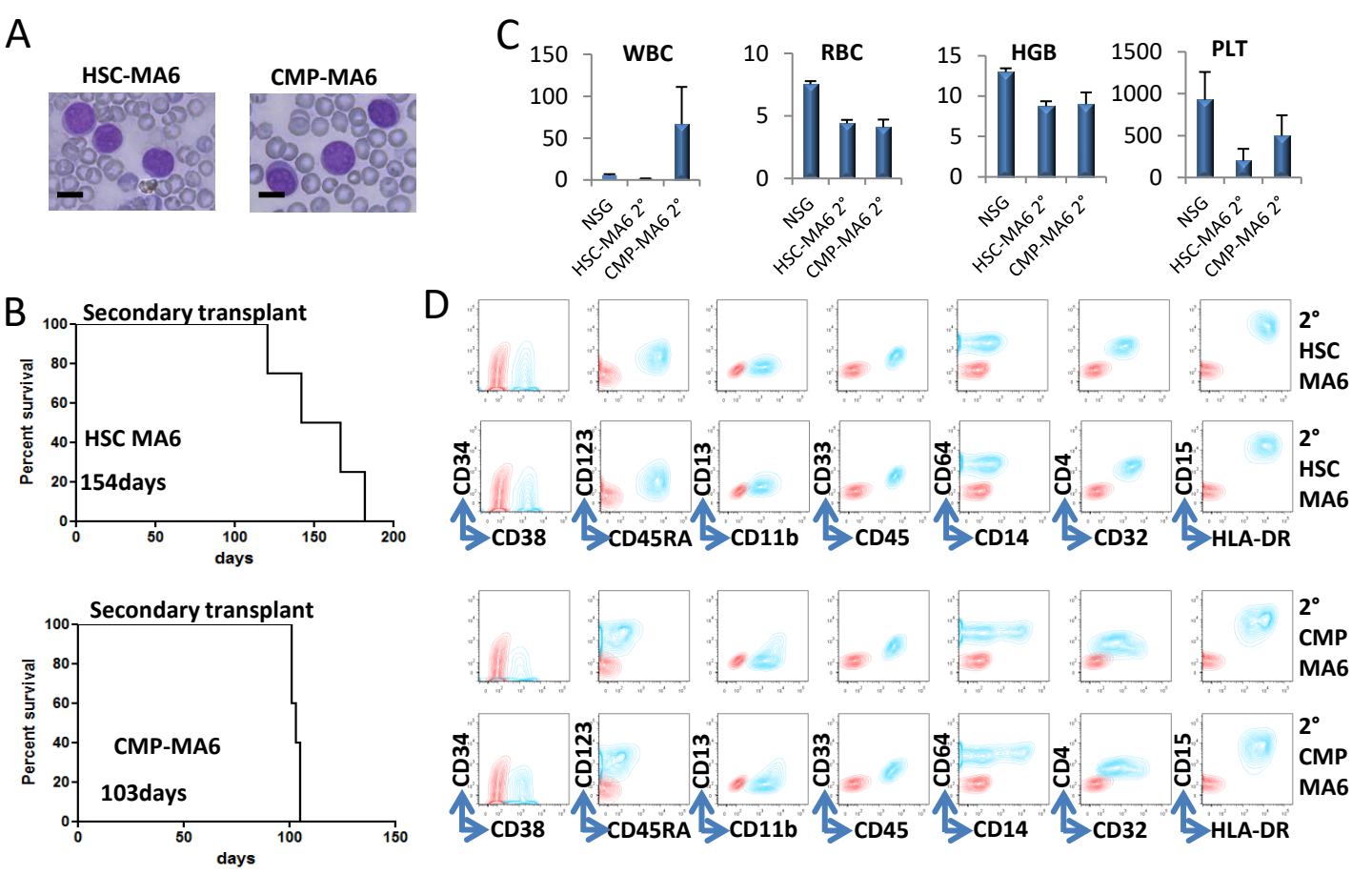
A
HSC-MA6
CMP-MA6
C
WBC
RBC
HGB
PLT
NSG
HSC-MA6 2°
CMP-MA6 2°
B
Secondary transplant
Percent survival
HSC MA6
154days
days
Secondary transplant
CMP-MA6
103days
days
D
2° HSC MA6
2° CMP MA6
CD34
CD38
CD123
CD45RA
CD13
CD11b
CD33
CD45
CD64
CD14
CD4
CD32
CD15
HLA-DR

A

CD34$^{-/lo}$ group:

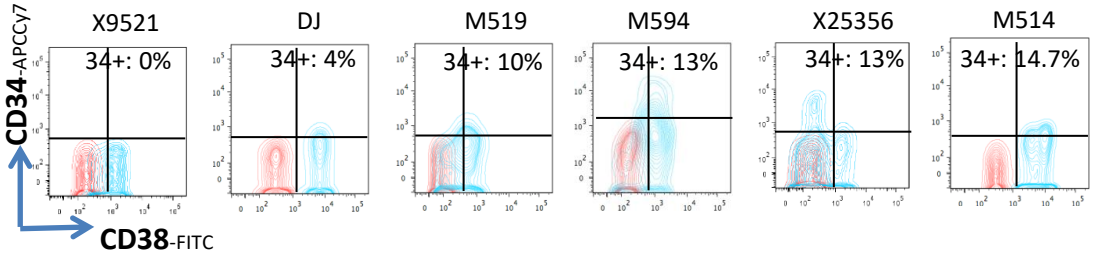

CD34^{+} group:

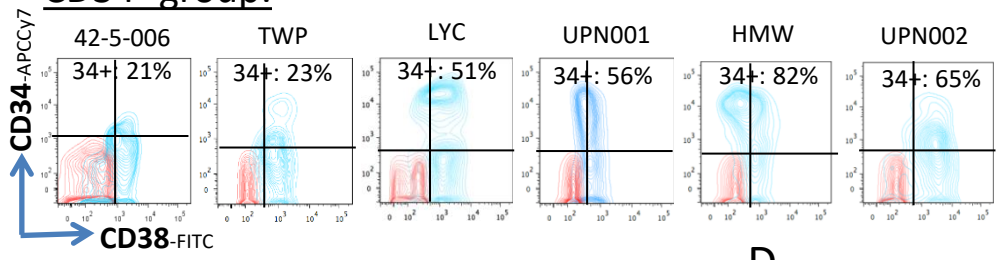

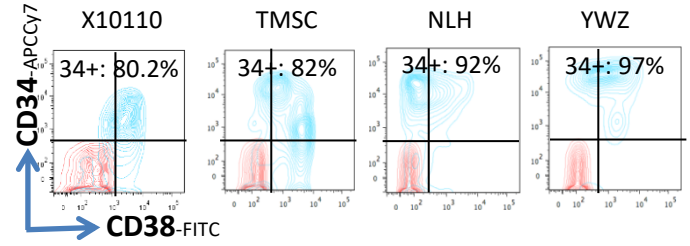

D

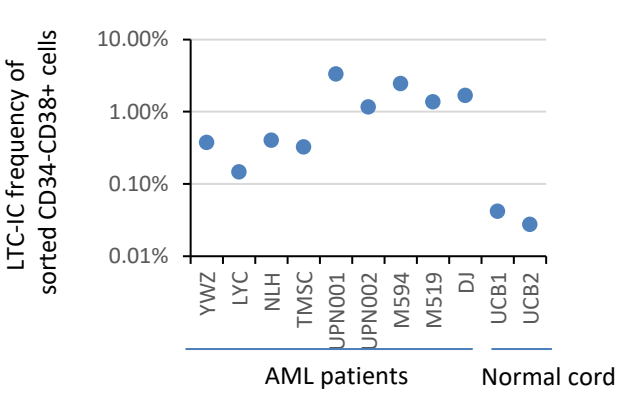

B

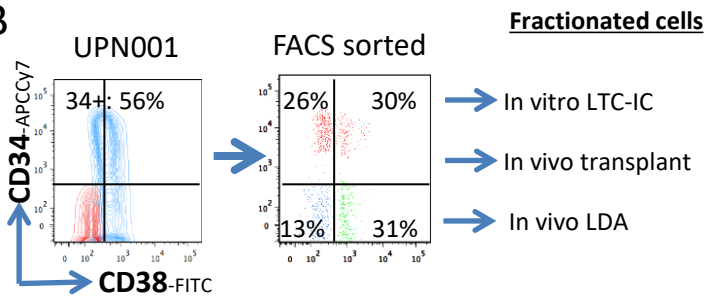

E

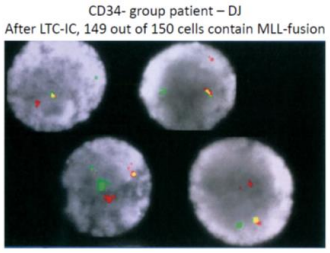

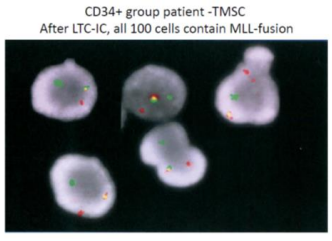

C

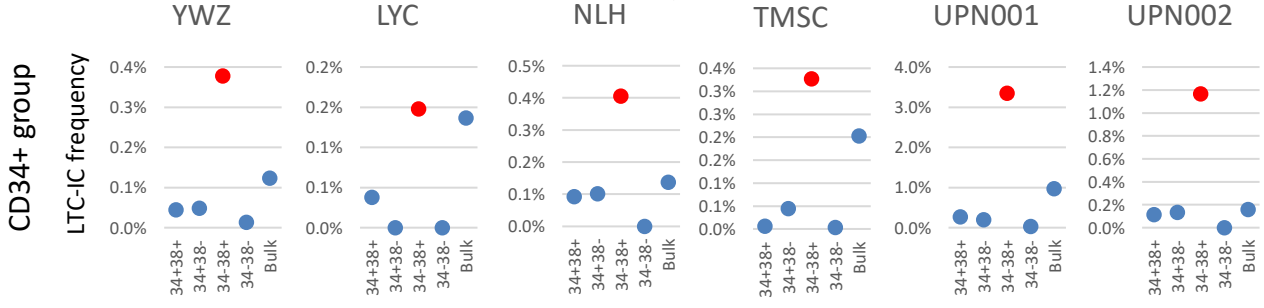

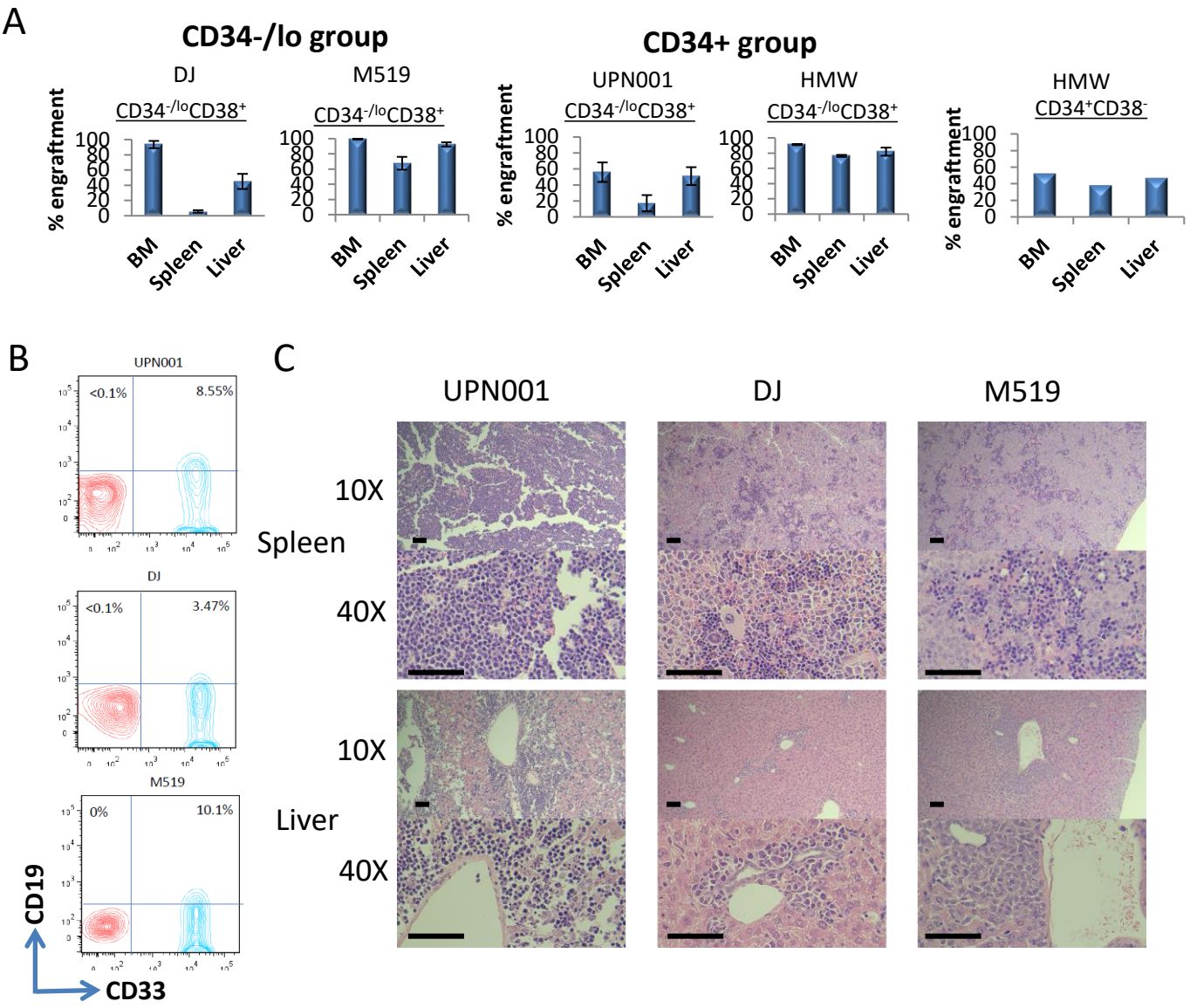
A
CD34-/lo group
CD34+ group
DJ
M519
UPN001
HMW
HMW
CD34-/loCD38+
CD34-/loCD38+
CD34-/loCD38+
CD34-/loCD38+
CD34+CD38-
% engraftment
% engraftment
100
80
60
40
20
0
BM
Spleen
Liver
B
UPN001
<0.1%
8.55%
DJ
<0.1%
3.47%
M519
0%
10.1%
CD19
CD33
C
UPN001
DJ
M519
10X
Spleen
40X
10X
Liver
40X

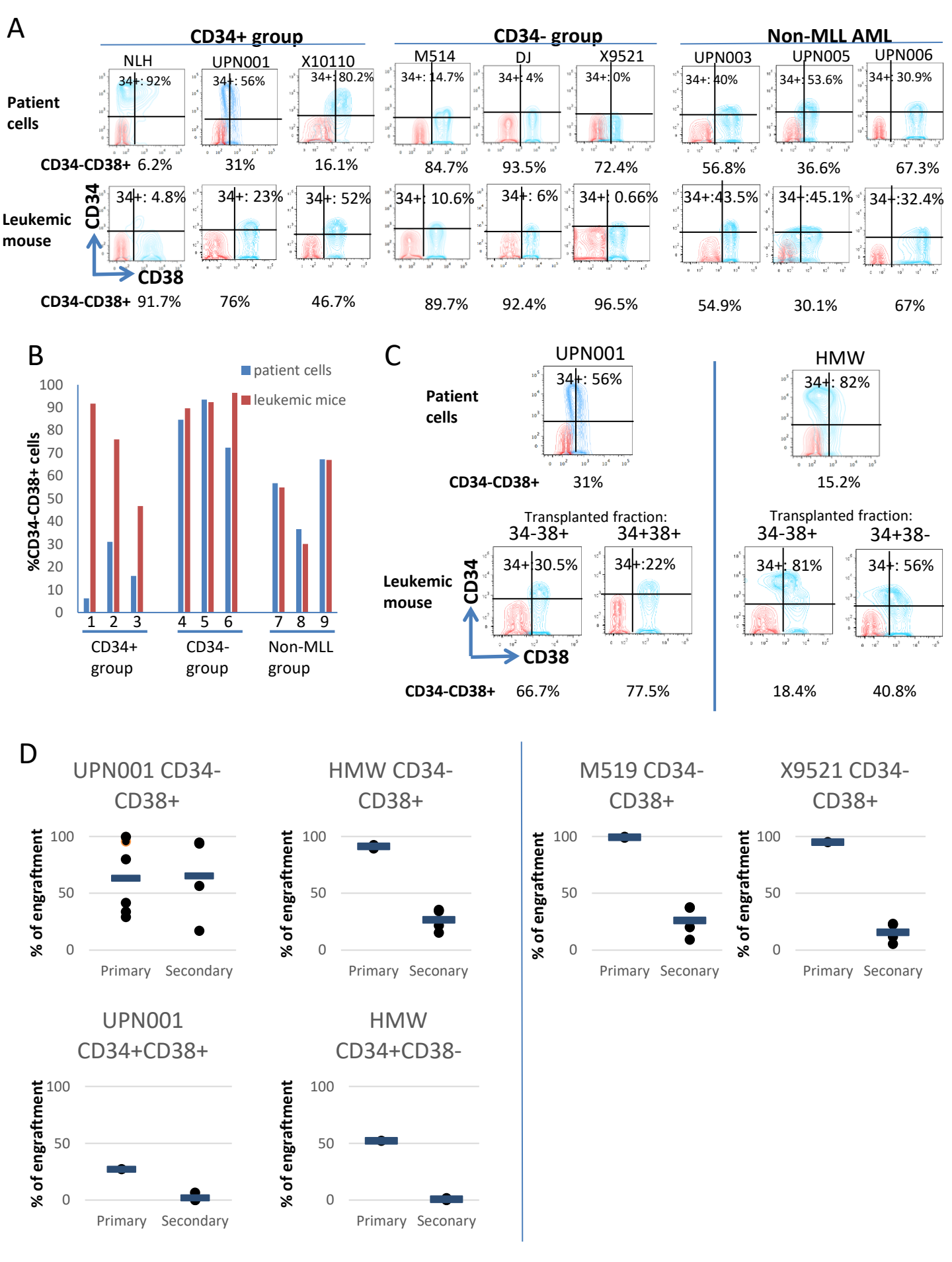
A
CD34+ group
CD34- group
Non-MLL AML
NLH
UPN001
X10110
M514
DJ
X9521
UPN003
UPN005
UPN006
Patient cells
34+: 92%
34+: 56%
34+: 80.2%
34+: 14.7%
34+: 4%
34+: 0%
34+: 40%
34+: 53.6%
34+: 30.9%
CD34-CD38+ 6.2%
31%
16.1%
84.7%
93.5%
72.4%
56.8%
36.6%
67.3%
Leukemic mouse
CD34
CD38
34+: 4.8%
34+: 23%
34+: 52%
34+: 10.6%
34+: 6%
34+: 0.66%
34+:43.5%
34+:45.1%
34+:32.4%
CD34-CD38+ 91.7%
76%
46.7%
89.7%
92.4%
96.5%
54.9%
30.1%
67%
B
patient cells
leukemic mice
%CD34-CD38+ cells
100
90
80
70
60
50
40
30
20
10
0
1 2 3
4 5 6
7 8 9
CD34+ group
CD34- group
Non-MLL group
C
UPN001
HMW
Patient cells
34+: 56%
34+: 82%
CD34-CD38+ 31%
15.2%
Transplanted fraction:
34-38+
34+38+
34-38+
34+38-
Leukemic mouse
CD34
CD38
34+: 30.5%
34+:22%
34+: 81%
34+: 56%
CD34-CD38+ 66.7%
77.5%
18.4%
40.8%
D
UPN001 CD34-CD38+
HMW CD34-CD38+
M519 CD34-CD38+
X9521 CD34-CD38+
% of engraftment
100
50
0
Primary
Secondary
Seconary
UPN001 CD34+CD38+
HMW CD34+CD38-

A

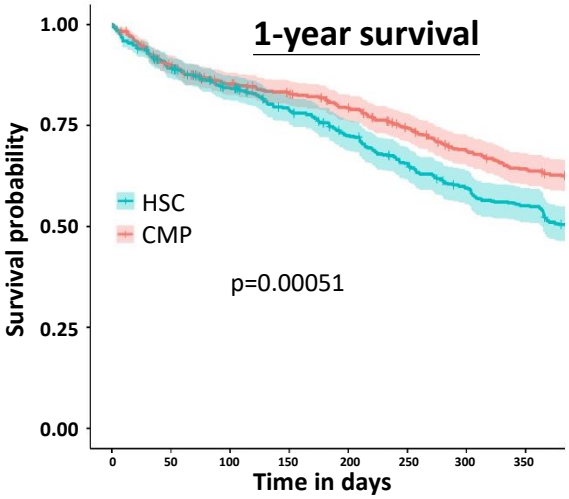
1-year survival
Survival probability
1.00
0.75
0.50
0.25
0.00
HSC
CMP
p=0.00051
0
50
100
150
200
250
300
350
Time in days

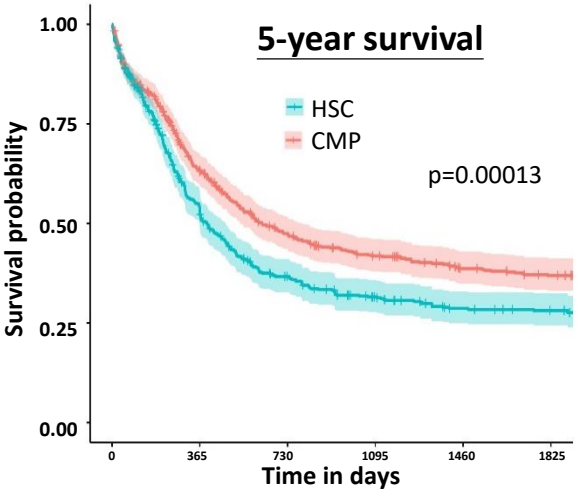
5-year survival
Survival probability
1.00
0.75
0.50
0.25
0.00
HSC
CMP
p=0.00013
0
365
730
1095
1460
1825
Time in days

B

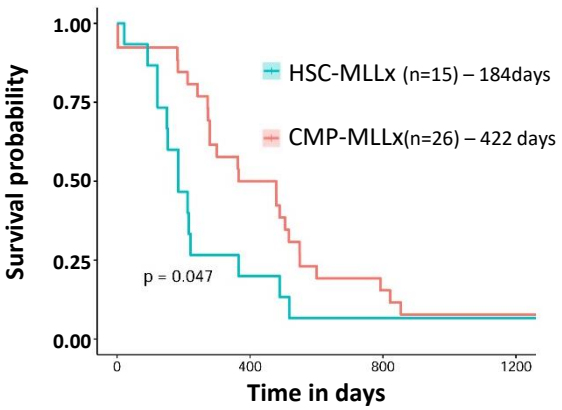
Survival probability
1.00
0.75
0.50
0.25
0.00
HSC-MLLx (n=15) – 184days
CMP-MLLx(n=26) – 422 days
p = 0.047
0
400
800
1200
Time in days

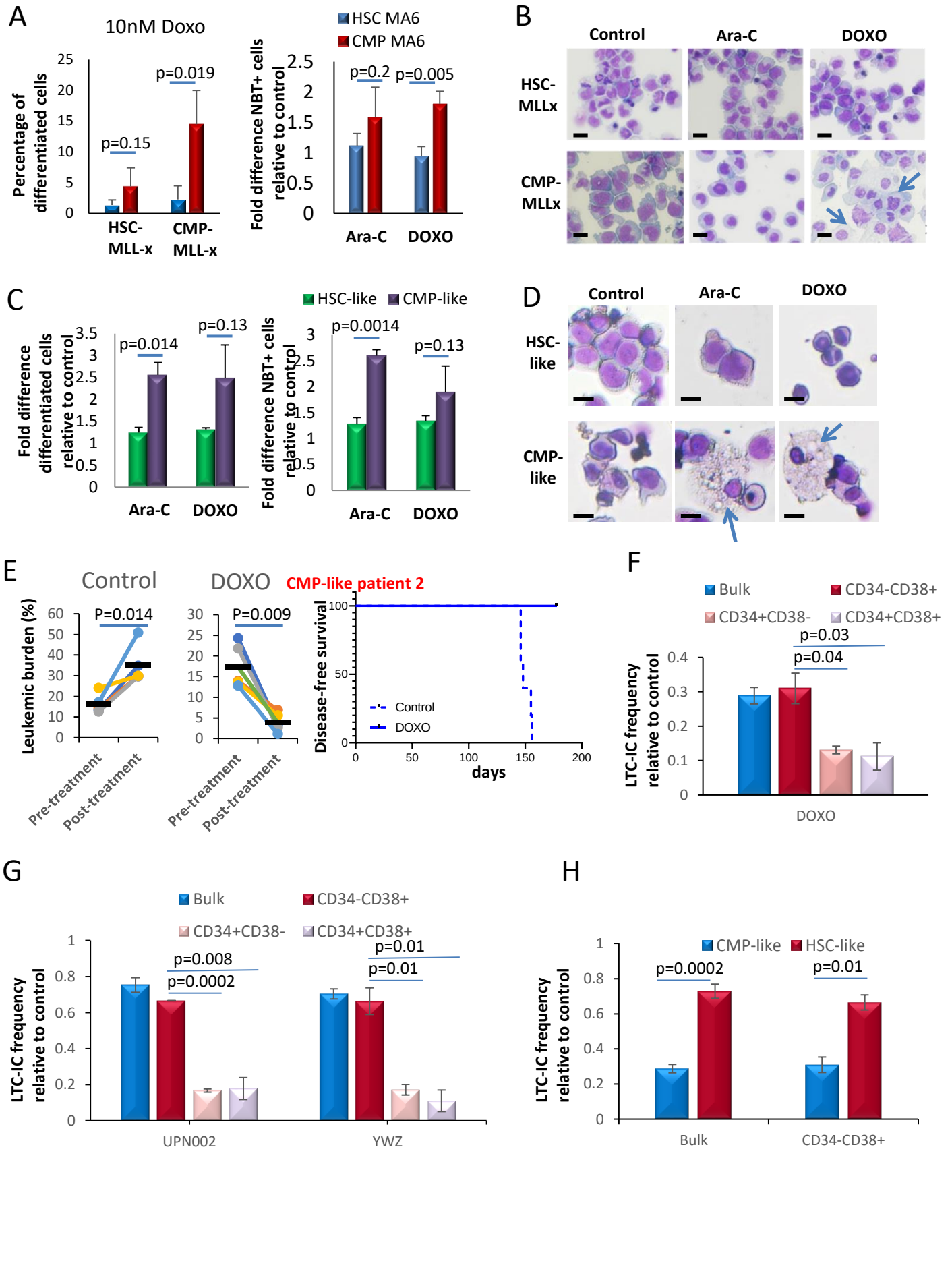
A
10nM Doxo
Percentage of differentiated cells
p=0.15
p=0.019
HSC-MLL-x
CMP-MLL-x
HSC MA6
CMP MA6
Fold difference NBT+ cells relative to control
p=0.2
p=0.005
Ara-C
DOXO
B
Control
Ara-C
DOXO
HSC-MLLx
CMP-MLLx
C
HSC-like
CMP-like
Fold difference differentiated cells relative to control
p=0.014
p=0.13
Fold difference NBT+ cells relative to control
p=0.0014
p=0.13
Ara-C
DOXO
D
Control
Ara-C
DOXO
HSC-like
CMP-like
E
Control
DOXO
CMP-like patient 2
Leukemic burden (%)
P=0.014
P=0.009
Pre-treatment
Post-treatment
Disease-free survival
Control
DOXO
days
F
Bulk
CD34-CD38+
CD34+CD38-
CD34+CD38+
LTC-IC frequency relative to control
p=0.03
p=0.04
DOXO
G
Bulk
CD34-CD38+
CD34+CD38-
CD34+CD38+
LTC-IC frequency relative to control
p=0.008
p=0.0002
p=0.01
p=0.01
UPN002
YWZ
H
CMP-like
HSC-like
LTC-IC frequency relative to control
p=0.0002
p=0.01
Bulk
CD34-CD38+

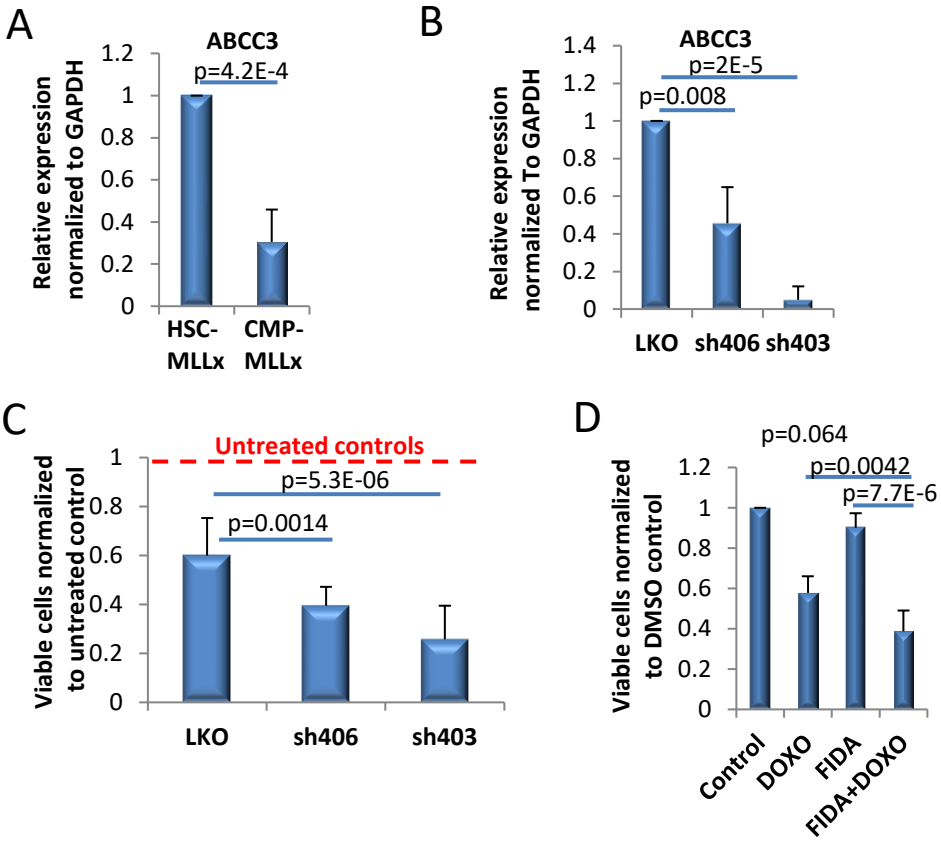
A
ABCC3
p=4.2E-4
Relative expression normalized to GAPDH
1.2
1
0.8
0.6
0.4
0.2
0
HSC-MLLx
CMP-MLLx
B
ABCC3
p=2E-5
p=0.008
Relative expression normalized To GAPDH
1.4
1.2
1
0.8
0.6
0.4
0.2
0
LKO
sh406
sh403
C
Untreated controls
p=5.3E-06
p=0.0014
Viable cells normalized to untreated control
1
0.8
0.6
0.4
0.2
0
LKO
sh406
sh403
D
p=0.064
p=0.0042
p=7.7E-6
Viable cells normalized to DMSO control
1.2
1
0.8
0.6
0.4
0.2
0
Control
DOXO
FIDA
FIDA+DOXO

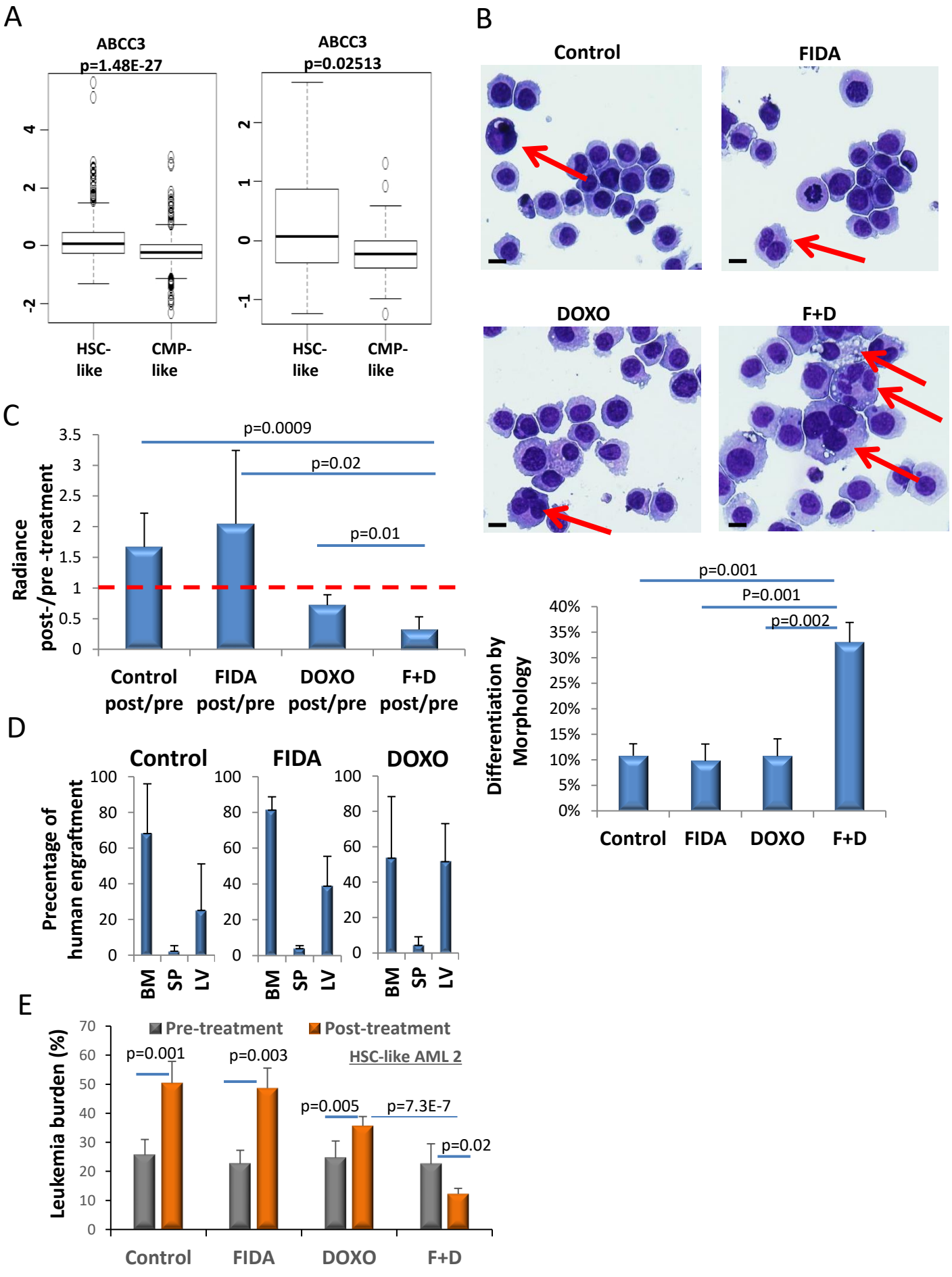
A
ABCC3
p=1.48E-27
ABCC3
p=0.02513
HSC-like
CMP-like
HSC-like
CMP-like
B
Control
FIDA
DOXO
F+D
C
Radiance post-/pre -treatment
p=0.0009
p=0.02
p=0.01
Control post/pre
FIDA post/pre
DOXO post/pre
F+D post/pre
Differentiation by Morphology
p=0.001
P=0.001
p=0.002
Control
FIDA
DOXO
F+D
D
Precentage of human engraftment
Control
FIDA
DOXO
BM
SP
LV
E
Leukemia burden (%)
Pre-treatment
Post-treatment
HSC-like AML 2
p=0.001
p=0.003
p=0.005
p=7.3E-7
p=0.02
Control
FIDA
DOXO
F+D

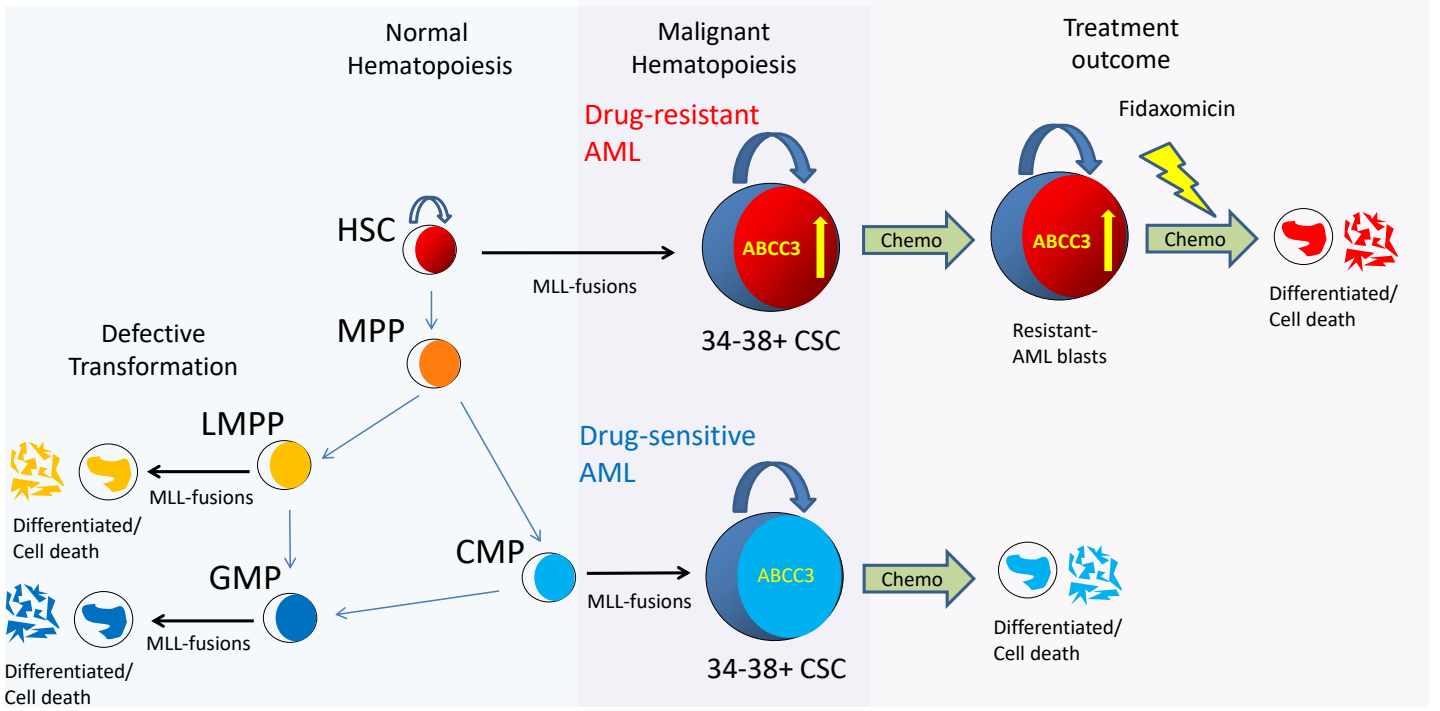
Normal
Hematopoiesis
Malignant
Hematopoiesis
Treatment
outcome
Drug-resistant
AML
Fidaxomicin
HSC
ABCC3
Chemo
ABCC3
Chemo
MLL-fusions
MPP
34-38+ CSC
Resistant-
AML blasts
Differentiated/
Cell death
Defective
Transformation
LMPP
Drug-sensitive
AML
MLL-fusions
Differentiated/
Cell death
CMP
ABCC3
Chemo
GMP
MLL-fusions
MLL-fusions
Differentiated/
Cell death
34-38+ CSC
Differentiated/
Cell death